NACA RM E54L23

NACA

RESEARCH MEMORANDUM

ANALYSIS OF A PRESSURE-JET POWER PLANT FOR A HELICOPTER

By Richard P. Krebs and William S. Miller, Jr.

Lewis Flight Propulsion Laboratory
Cleveland, Ohio

CLASSIFICATION CHANGED

UNCLASSIFIED

NACA Res abs

By authority of ▼KN-123 Date effective Dec. 1957

AMT 1- 2055

NATIONAL ADVISORY COMMITTEE
FOR AERONAUTICS
WASHINGTON
March 28, 1955

NATIONAL ADVISORY COMMITTEE FOR AERONAUTICS

RESEARCH MEMORANDUM

ANALYSIS OF A PRESSURE-JET POWER PLANT FOR A HELICOPTER

By Richard P. Krebs and William S. Miller, Jr.

SUMMARY

An analysis of a pressure-jet power plant for a helicopter was made at the Lewis laboratory to determine suitable values for the principal power-plant design parameters. Pressure ratio of the auxiliary compressor, tip-jet temperature, burner area, blade-duct area, and rotor tip speed were varied; the effects of these variations on power-plant specific thrust and thrust specific fuel consumption are presented. Comparison of a series of pressure-jet power plants installed in an assumed helicopter of 30,000 pounds gross weight is presented on the basis of calculated hovering duration and flight range.

Specific thrust of the pressure-jet power plant was found to increase with increasing pressure ratio of the auxiliary compressor and with increasing jet temperature. For jet temperatures lower than about 2200° R, thrust specific fuel consumption improved with decreasing pressure ratios. For jet temperatures between 2200° and 4000° R, thrust specific fuel consumption improved with increasing pressure ratios. When blade-duct Mach numbers were low, system pressure losses due to blade-duct friction and momentum pressure losses in the tip burners had an insignificant effect on specific thrust. At high duct Mach numbers, duct friction losses and burner momentum losses (unchoked burner) had nearly equal effects on specific thrust.

Comparison of a series of pressure-jet power plants installed in a 30,000-pound helicopter demonstrated that flight performance in hovering and forward flight was poor at low design jet temperatures and low design pressure ratios when the blade-duct area was 30 percent and the burner area was 45 percent of the blade-section area. Significant improvement in flight performance was obtained at low design jet temperatures when the duct area was increased to 50 percent of the section area and the burner area was increased to 75 percent of the section area; only small gains, however, were realized at best design temperatures and pressure ratios. Because of higher thermal and propulsive efficiencies, the variable-area tip-nozzle configuration gave marked flight performance superiority over the fixed-area nozzle configuration. Helicopter gross weight had no significant influence on the choice of optimum power plant for fixed rotor geometry.

3355

INTRODUCTION

The design and operational advantages inherent to the jet-driven helicopter rotor are well known. In comparison with the shaft-driven rotor, the jet rotor is shown in references 1 and 2 to provide direct reductions in helicopter empty weight and to increase the pay-load capacity by (1) eliminating the gear-reduction train between the rotor shaft and the power plant, (2) eliminating the antitorque tail rotor, and (3) using a power plant of low specific weight.

In other analyses (ref. 3, e.g.) the performance characteristics that are unique to several different tip-mounted power plants are examined. Although heavier than the ram jet or pulse jet, the pressure jet with tip burning is shown to be particularly applicable to large helicopters because of its characteristic high unit thrust. With the pressure jet, rotor performance is not significantly impaired by the external drag of excessively large tip units. Furthermore, the pressure jet is not subject to the high-tip-speed limitations of the pulse jet nor to the ram-recovery problems of either pulse jet or ram jet resulting from large variations in inlet angle of attack.

As part of a program devoted to the study of jet propulsion as applied to helicopters, an analysis of the pressure-jet power plant was made at the NACA Lewis laboratory in order to determine suitable values for the primary design parameters of the pressure-jet system. The pressure ratio of the auxiliary compressor and the tip-jet temperature were varied, and the effects on pressure-jet performance were calculated. Several additional parameters having a significant effect on pressure-jet performance, namely, duct area, burner area, and rotor tip speed, were also varied; the effects on power-plant performance were determined. Many of the design parameters that affect power-plant performance (e.g., tip speed) also affect helicopter rotor performance. Therefore, in order to determine the over-all effects of variation in power-plant parameters on the combined system performance, the flight performance of an assumed pressure-jet helicopter was investigated. The performance of a series of pressure-jet power plants is, however, presented separately from that of the combined system, and a comparison of power-plant performance is made on the basis of calculated net specific thrust and net thrust specific fuel consumption.

Inasmuch as helicopter weight and rotor power requirements decrease continuously during flight, a corresponding reduction in the power output of the pressure-jet system must be made. In this analysis, operation of the pressure-jet power plant was investigated for the design-point and for part-load or off-design-point conditions. From the assumed helicopter configuration, an off-design power schedule for the power plant was calculated, and practical values for blade-duct and

tip-burner areas were determined. Performance of a series of pressure-jet power plants installed in a helicopter of fixed gross weight was investigated for two flight plans, comparison being made on a basis of calculated duration in all-hovering flight and range in forward flight.

ASSUMPTIONS AND ANALYSIS

Description of Pressure-Jet System

The pressure-jet system investigated herein is shown schematically in figure 1. A gas-turbine engine of the turboprop type was assumed direct-coupled to an auxiliary compressor that provides compressed air to the tip burners. The auxiliary compressor rotates at the gas-turbine shaft speed, thereby eliminating the integral reduction gear of the turboprop engine. Air from the compressor is ducted to the rotor hub and out through the blade ducts to combustion chambers at the blade tips where additional fuel is burned. Reaction from the tip jets furnishes the torque to drive the rotor. No assist in forward flight was assumed from the jet thrust of the gas-turbine engine. The location of the pressure-jet components in the assumed helicopter is given in figure 2.

Gas-Turbine Engine

The gas turbine used to drive the auxiliary compressor was assumed typical of current turboprop engines in the 2000- to 3000-horsepower class. Reference 4 shows that, for an engine of this type, horsepower per unit air flow is relatively constant for pressure ratios from 6.0 to 8.0 at a turbine-inlet temperature of 2000° R. From the standpoint of power-plant simplicity and to ensure low power-plant weight, a single-spool compressor with a pressure ratio of 6.0 was assumed. No attempt was made in the analysis to optimize the gas-turbine design parameters for specific pressure-jet installations. Fuel consumption of the gas turbine was a function of shaft horsepower output and shaft speed and is given graphically in figure 3. Specific weight of the gas turbine plus auxiliary compressor was based on an estimated gas-turbine weight of 0.75 pound per shaft horsepower, minus 0.25 (lb/shp) for the gear reduction box, plus 0.15 (lb/shp) for the auxiliary compressor, giving a total specific weight of 0.65 pound per shaft horsepower for gas turbine plus auxiliary compressor. The sensitivity of helicopter flight performance to engine weight was determined by arbitrarily increasing the assumed specific weight from 0.65 to 1.0 (lb/shp) and recomputing the hovering time for one pressure-jet configuration.

Auxiliary Compressor

The auxiliary compressor assumed herein is representative of present-day, high-performance, axial-flow compressors. Compressor characteristics, shown in figure 4, are assumed independent of design pressure ratio and design weight flow. Discussion of off-design operation along the compressor operating line, drawn through the maximum efficiency plateau in figure 4, is given in appendix A. The effect of small changes in compressor efficiency on flight performance was investigated.

Tip Burners and Blade Ducts

Experimental investigations reported in reference 5 indicate that extreme centrifugal accelerations may decrease the combustion efficiencies of tip-mounted combustors by distorting the fuel-spray pattern. When accelerations are not greatly in excess of 400g's, however, combustion efficiencies nearly equal to those in a static burner are attainable. Except for the highest tip speed investigated, that is, 900 feet per second, accelerations of the tip burners considered herein are less than 400g's and a combustion efficiency of 0.90 is assumed. The assumed jet nozzle velocity coefficient is 0.95.

Burner areas may often be limited by profile-drag considerations of the helicopter rotor. The faired two-dimensional tip burner is preferable to the circular burner from the standpoint of low rotor drag and is therefore assumed herein. Burner areas were varied over a range from 45 to 75 percent of the assumed helicopter rotor-blade section area and, because the burner is completely faired into the tip airfoil section, no corrections for external drag were made to the rotor power calculations.

Selection of blade-duct areas for the pressure-jet system will often require that a compromise be made between the low-pressure-drop requirements of the pressure-jet power plant and the low-profile-drag requirements of the helicopter rotor. The blade-duct area, for instance, must be large enough to supply compressed air to the tip burners without excessive friction pressure drop and, at the same time, be of a practical size in view of current blade design and fabrication procedures. In this analysis, two duct sizes were considered: (1) a duct having an area equal to 30 percent of the rotor-blade section area, and (2) a duct having an area equal to 50 percent of the section area. The smaller duct appears entirely realistic with existing blade profiles and construction methods, while the larger duct may require some modification of current design practice.

3355

Cycle Calculations

The analysis of the pressure-jet cycle, which included the usual cycle losses, considered the following: (1) inlet diffuser losses, (2) compressor efficiency, (3) friction losses, (4) pumping work for air and fuel in the blades, (5) momemtum pressure losses in the tip burners, (6) tip-burner combustion efficiency, and (7) tip-burner exhaust-nozzle efficiency. For the major part of the analysis, the friction pressure loss was assumed to equal 2.5 times the dynamic pressure in the blade duct. This friction-loss factor, discussed in more detail in appendix A, includes the friction losses of the fuselage duct, blade ducts, turning elbows, and combustor flameholders. Burner momentum pressure loss was calculated as a function of burner Mach number and combustor temperature ratio. In the analysis the ratio of burner area to duct area was varied from 1.5 to 2.5 in order to show the effects of burner momentum pressure losses on power-plant specific thrust. The effects on helicopter flight performance due to system pressure losses were studied by varying independently the physical areas assigned to the blade ducts and to the tip burners.

In the cycle calculations, design pressure ratio and design jet temperature were selected and net thrust per unit air flow was computed for a range of duct Mach numbers. Results were plotted as net thrust per unit air flow against net thrust per unit duct area for a given pressure ratio, tip speed, and ratio of burner area to duct area. In the typical power-available chart shown in figure 5(a), dashed lines connect points of constant tip-jet temperature and solid lines connect points of constant duct Mach number. Details of the cycle calculations are given in appendix A.

Range of Pressure-Jet Variables

The pressure-jet parameters were varied through the following ranges:

(1) Pressure ratio of auxiliary compressor, 2.25 to 5.0

(2) Tip-jet temperature, compressor-discharge temperature to 4000° R

(3) Ratio of duct area to section area, 0.3 to 0.5

(4) Ratio of burner area to section area, 0.45 to 0.75

(5) Rotor tip speed, 500 to 900 feet per second

Off-Design Operation of Pressure-Jet Power Plant

Design values for auxiliary-compressor pressure ratio, tip-jet temperature, and air flow were matched for initial hovering-power requirements at maximum helicopter gross weight. A reduction in the power output of the pressure-jet system is required as fuel is consumed and the helicopter weight decreases. Cruise flight represents another part-load condition for the power plant. Two methods of off-design operation of the pressure-jet system were considered in this analysis. The first method, used for the major part of the analysis, assumed a variable-area tip-jet nozzle; the second method assumed a fixed-area tip-jet nozzle.

In off-design operation with the variable-area nozzle, the gas turbine and the auxiliary compressor are held at design values of speed, pressure ratio, and air flow, while the fuel flow to the tip burner and the tip-jet nozzle area are reduced as the power requirements decrease. In off-design operation with the fixed-area nozzle, speed, pressure ratio, and air flow of the auxiliary compressor are reduced along the operating line of figure 4 and fuel flow to the tip burners is decreased, thereby reducing the power output of the pressure-jet system. Further discussion of the off-design condition is given in appendix A.

Reserve Power

Helicopter reserve power is assumed herein to be 20 percent higher than design hovering power. With the variable-area jet nozzle, reserve power is developed when the jet temperature is raised above the design value, with the pressure ratio and air flow remaining constant. Because 4000° R is the stoichiometric limit for tip-jet temperatures, design jet temperatures were restricted to values low enough to provide the necessary 20 percent reserve power at the stoichiometric limit. With the fixed-area nozzle, the gas turbine is assumed to run at 90 percent rated speed in initial hovering flight, and reserve power is developed when the gas-turbine speed is raised to rated value. The resulting increase in auxiliary-compressor pressure ratio and weight flow provides the necessary reserve power for the helicopter.

HELICOPTER CONFIGURATION

A criterion for the aerodynamic efficiency of the jet-driven helicopter rotor is defined in reference 6 as the ratio of rotor thrust generated in hovering flight T to the tip-jet thrust required F_n. Constant values for rotor solidity σ, mean lift coefficient $\overline{C}_L$, and thrust coefficient C_T are shown to give constant values for the efficiency ratio T/F_n. These rotor design parameters were therefore fixed

for the major part of this analysis, providing a rotor of constant efficiency for flight performance comparisons of the pressure-jet helicopters. Combinations of tip speed, disk loading, and solidity used herein are considered representative of present-day practice for helicopters in the 30,000-pound class. Because comparative rather than absolute flight performance was of primary interest, no attempt was made to optimize the rotor aerodynamic parameters. The degree to which changes in the helicopter configuration may affect power-plant selection is discussed in RESULTS AND DISCUSSION.

The following summarizes the fixed parameters of the assumed helicopter:

General:

Gross weight, W_g, lb 30,000
Number of rotors 1
Number of blades, b 2
Fuselage flat-plate area, A_p, sq ft 36
Structure weight . . . . (appendix B)

Rotor:

Blade airfoil section . . . . 64_1-012 (smooth)
Type of blade . . . . Twisted, untapered
Blade twist, deg . . . . -12
Blade mean lift coefficient, $\bar{C}_L$ 0.42
Rotor solidity, σ 0.073
Tip loss factor, B . . . . (ref. 7)
Design thrust coefficient, C_T 0.0051

The assumption of constant rotor solidity and constant thrust coefficient is shown in appendix B to fix the following relations between tip speed, disk loading, rotor diameter, and blade chord:

Tip speed, ft/sec	Disk loading, lb/sq ft	Rotor diameter, ft	Chord, ft	Structure weight / Gross weight	Blade-section area, sq ft
500	3.05	112.0	6.44	0.405	2.678
600	4.40	93.4	5.37	.380	1.859
700	6.00	80.0	4.60	.360	1.368
900	9.90	62.2	3.58	.327	.828

Tabulated values of the ratio of structure weight to gross weight are functions of the rotor diameter and disk loading. Blade-section

areas for the 64_1-012 airfoil are tabulated since duct and burner areas
will be given in RESULTS AND DISCUSSION as percentages of the section
area.

Flight Plans

Helicopter flight performance was calculated for two different
flight plans. One plan consisted of all-hovering flight out of the
ground effect at standard sea-level conditions. The other plan con-
sisted of forward flight at 83 knots at a pressure altitude of 5000
feet but at an ambient temperature corresponding to sea level. The
speed of 83 knots corresponds to a tip-speed ratio μ of 0.2 at a
tip speed of 700 feet per second. An outline of the calculations
giving helicopter power-required curves for these flight plans is
given in appendix B.

Flight Performance Calculations

During any flight operation, the helicopter gross weight continu-
ously decreases as fuel is burned. Power requirements and fuel-
consumption rate also decrease continuously. In order to compute hov-
ering time and range for those flights in which the entire useful load
is fuel, the fuel load was divided into six equal increments and the
power required and the fuel consumption rate were computed for the av-
erage gross weight of the helicopter in each of the six increments. Ro-
tor power requirements were calculated from rotor performance curves de-
scribed in appendix B. Weight of the fuel tanks was assumed equal to
0.1 of the total fuel weight. For most cases with variable-area nozzle
operation, fuel consumption of the gas turbine is constant during flight
and was computed from the required compressor horsepower and the
specific-fuel-consumption curves of figure 3. The tip-jet temperatures
for each power requirement were found from operating lines similar to
that shown in figure 5(h); corresponding tip-burner fuel flows were
found from the charts of reference 8. The six incremental flight times
were determined by dividing the incremental fuel weight by the sum of
the instantaneous fuel rates for the gas turbine and tip burners. The
total flight duration is equal to the sum of the time increments, and
flight range is total flight time multiplied by the flight speed.

RESULTS AND DISCUSSION

The performance of the pressure-jet power plant and the performance
of the power-plant - helicopter combination are separately presented.
In the first section specific thrust and thrust specific fuel consump-
tion for a series of pressure-jet power plants are given. The second

section compares the performance of the same series of pressure-jet power plants on a basis of calculated hovering time and flight range for the assumed helicopter.

Power-Plant Performance

Power-available charts. - Results of the cycle calculations for the variable-area tip-nozzle pressure jet are presented graphically in figures 5(a) to (p). In this series of power-available charts, performance of the pressure-jet system is given for a range of tip speeds from 500 to 900 feet per second; for each tip speed, a range of pressure ratios is given, for example, 2.25 to 5.0 at a tip speed of 700 feet per second. At a pressure ratio of 2.5 and a tip speed of 700 feet per second, the ratio of the burner area to the duct area is varied from 1.5 to 2.5.

A representative power-available chart for a fixed-area tip-nozzle pressure jet is given in figure 5(q). Here, net thrust per unit duct area and jet temperature are plotted against coordinates of compressor pressure ratio and air flow per unit duct area.

These power-available charts can be extended, if desired, by the equations of appendix A to higher values of thrust per unit duct area for the variable-area configuration and, for the fixed-area configuration, charts can be constructed for additional ratios of nozzle area to duct area.

Effects of system pressure drop on pressure-jet performance. - System pressure drop, resulting from blade-duct friction losses and tip-burner momentum losses, decreases the net specific thrust as duct Mach numbers increase. This effect is demonstrated by the downward slope of the constant jet temperature lines with increasing duct Mach number (fig. 5) and is particularly evident in the performance charts for the low pressure ratios (2.25 and 2.5). For low pressure ratios, a given system pressure drop represents a larger proportion of the available pressure than with the higher pressure ratios. At a pressure ratio of 2.5 and a jet temperature of 3000° R (fig. 5(h)), specific thrust is nearly constant for duct Mach numbers less than 0.14. In general, neither friction pressure losses in the blade ducts nor momentum pressure losses in the tip burners have a significant effect on pressure-jet performance when M_x is low. However, at 3000° R, specific thrust is reduced approximately 18 percent when M_x is increased from 0.14 to 0.34, showing the influence of both duct friction and burner momentum pressure losses. The individual effects of these two sources of system pressure drop are illustrated in figure 6.

In figure 6, the bottom curve has been redrawn from figure 5(h) and gives specific thrust for a jet temperature of 3000° R and a pressure ratio of 2.5 when both duct friction and burner momentum losses are included. The middle curve presents specific thrust as a function of M_x for assumed zero momentum pressure loss in the burner and duct friction loss equal to 2.5 times the dynamic pressure in the blade duct. For an increase in M_x from 0.14 to 0.34, specific thrust is reduced about 9 percent. The top curve gives specific thrust for the alternate case where duct friction losses are neglected and burner losses are computed from burner Mach numbers and temperature ratio. Specific thrust is reduced about 7 percent in this case for an increase in M_x from 0.14 to 0.34. Comparison of the three curves indicates that, for the temperature ratio given, duct and burner pressure losses contribute about equally to thrust reduction at M_x of 0.34. Further increases in duct Mach numbers will raise burner Mach numbers to thermal choking values, causing specific thrust to decrease very rapidly. The condition of thermal choking in the tip burner can be delayed to higher duct Mach numbers by increases in the combustion-chamber area. This effect is illustrated by a comparison of figures 5(h) and (j), in which the ratios of burner area to duct area are 1.5 and 2.5, respectively. For the smaller burner, figure 5(h) shows a specific-thrust reduction of 18 percent for an increase in M_x from 0.14 to 0.34. Figure 5(j), on the other hand, gives the specific-thrust reduction as only 10 percent for the same increase in M_x, illustrating the performance benefits accruing to the larger burner.

Specific thrust as function of pressure ratio and jet temperature. - The specific thrust of the pressure-jet system is plotted as a function of pressure ratio and jet temperature in figure 7(a). The data for this plot were obtained from the power-available charts for an assumed duct Mach number of 0.1. At this Mach number specific thrust is not significantly affected by system pressure losses. Horsepower developed by the pressure jet at a rotor tip speed of 700 feet per second is given in figure 7(b). The figures show that both specific thrust and rotor horsepower per unit air flow increase with increasing pressure ratio and jet temperature.

Gas-turbine horsepower and fuel consumption. - Because the gas turbine is direct-coupled to the auxiliary compressor, gas-turbine horsepower equals auxiliary-compressor horsepower and, for constant compressor efficiency, is independent of tip-jet temperature and rotor tip speed. Gas-turbine horsepower required per unit air flow through the pressure-jet system is given as a function of auxiliary-compressor pressure ratio in figure 8(a). From the assumed gas-turbine design-point specific fuel consumption of 0.74 pound per horsepower-hour and from the data of figures 7(a) and 8(a), the gas-turbine thrust specific fuel consumption was calculated as a function of auxiliary-compressor pressure ratio and jet temperature and is plotted in figure 8(b).

3355

CQ-2 back

Specific fuel consumption of pressure-jet power plant. - Thrust specific fuel consumption for the tip burners is given as a function of jet temperature and pressure ratio in the lower set of curves in figure 9. Intersections of the tip-burner specific-fuel-consumption curves with the horizontal axis indicate the "cold-jet" condition where no fuel is burned in the tip combustors.

Total thrust specific fuel consumption of the pressure-jet power plant is equal to the sum of the specific fuel consumption of the tip burners and the specific fuel consumption of the gas turbine. Total thrust specific fuel consumption of the power plant, plotted as a function of jet temperature and pressure ratio, is given in the upper set of curves in figure 9. In the jet temperature range from 2500° to 4000° R, specific fuel consumption for the pressure-jet power plant is best for the higher pressure ratios. For jet temperatures in the lower ranges, specific fuel consumption is best for the lower pressure ratios, with cross-over of the specific-fuel-consumption curves occurring in the range of temperatures between 1500° and 2250° R. Subsequent discussion will show that this cross-over of the specific-fuel-consumption curves is a factor that influences the choice of power plant for the assumed pressure-jet helicopter.

Effect of rotor tip speed on power-plant performance. - Specific thrust developed by the pressure jet is plotted as a function of rotor tip speed in figure 10(a) for a pressure ratio of 3.0 and a jet temperature of 3500° R. Increased pumping work for air and fuel in the rotor blades reduces specific thrust 6 percent when the tip speed is increased from 500 to 900 feet per second. This advance in tip speed is shown to increase the rotor horsepower developed 60 percent (fig. 10(b)) and increase thrust specific fuel consumption for gas turbine plus tip burner 13 percent (fig. 10(c)).

Effects of Power-Plant Design Parameters on Flight Performance

Auxiliary-compressor pressure ratio and tip-jet temperature. - The flight performance of the assumed 30,000-pound helicopter with a series of pressure-jet power plants is given in figure 11. Here, hovering time and flight range are plotted as functions of design jet temperature for design pressure ratios from 2.25 to 5.0. Power-plant design coordinates, pressure ratio and jet temperature, are defined at the maximum-gross-weight hovering-power condition and, in each case, hovering time and flight range are given for a fuel load equal to the useful load of the helicopter. Minimum areas were assumed in this case for the blade ducts and tip burners, that is, blade-duct area was 30 percent and burner area was 45 percent of the blade-section area. Rotor tip speed was 700 feet per second.

For this configuration, hovering time is maximum (5.45 hr) at a
pressure ratio of 3.0 and is nearly independent of design jet temper-
atures in the range from 2100° to 4000° R. Forward flight range is
maximum (730 nautical miles) at a pressure ratio of 3.0 and a design
jet temperature of 4000° R. A design-jet-temperature-limit line was
drawn at 3000° R to indicate the highest jet temperature that will
provide a reserve power 20 percent above hovering power when jet tem-
peratures are raised in flight to the stoichiometric limit of 4000° R.

Pressure ratios higher than 3.0 are shown in figure 11 to give re-
duced hovering times and flight ranges, hovering time dropping 9 percent
and range nearly 10 percent when the design pressure ratio is increased
from 3.0 to 5.0 at the design jet temperature of 3000° R. This perform-
ance trend is due in part to the lower power-plant weight of the low-
pressure-ratio system, the system with a pressure ratio of 3.0 weighing
approximately 25 percent less than the system with a pressure ratio of
5.0. This difference in power-plant weight, due to the greater fuel
load carried, accounts for one-half of the difference in hovering time
for the two pressure ratios. The superiority in specific fuel consump-
tion for the lower-pressure-ratio system explains the remaining differ-
ence in flight duration. Reference to figure 9, however, which gives
power-plant specific fuel consumption as a function of pressure ratio
and temperature, reveals an apparent contradiction to this statement.
In that figure the 5.0-pressure-ratio system is shown to have slightly
superior specific fuel consumption to that for the lower-pressure-ratio
system at a jet temperature of 3000° R. The apparent contradiction is
explained by consideration of jet temperature as a function of elapsed
flight time for the two pressure ratios.

In figure 12, jet temperature is plotted against elapsed hovering
flight time for pressure ratios of 3.0 and 5.0 and for the design jet
temperature of 3000° R. Because variable-area operation of the tip
nozzle is assumed, tip-jet temperatures decrease continuously as the
flight progresses. The curves show that jet temperatures are reduced
below 2000° R after 1.4 hours of hovering flight. In figure 9, a jet
temperature of 2000° R is the cross-over point for the specific-fuel-
consumption curves at pressure ratios of 3.0 and 5.0; for lower temper-
atures, the 3.0-pressure-ratio system has the better specific fuel
consumption.

Figure 11 shows that hovering time drops off sharply as design jet
temperatures are decreased at design pressure ratios of 2.25 and 2.5.
Reference to the applicable power-available chart (fig. 5(g)) for a
pressure ratio of 2.25 shows that this effect is a result of increased
momentum losses in the tip burners and increased friction losses in the
blade ducts. From the equations of appendix B, the design value of net
thrust required per unit duct area was calculated as 2600 pounds per
square foot for the 30,000-pound helicopter with a tip speed of 700 feet

3355

per second. In figure 5(g), intersections of the vertical line, drawn at 2600 pounds per square foot on the horizontal axis, with the 4000° and 3500° R jet temperature lines occur at high values of M_x, where specific thrust is decreasing rapidly. At M_x of 0.34, the 3000° jet temperature line has a nearly vertical slope and has no intersection with the design F_n/A_x line. As indicated in figure 11, hovering flight at maximum gross weight was impossible at a design pressure ratio of 2.25 and a design jet temperature of 3000° R, because the required thrust was not developed by the pressure-jet power plant.

Tip-burner area. - Hovering time and flight range are plotted against design jet temperature in figure 13 for the previously shown burner size of 45 percent of the blade-section area and for two larger burners of 60 and 75 percent of the section area. For these results, the blade-duct area was fixed at 30 percent of the section area and the design pressure ratio was 2.5. With the 45-percent burner, thermal choking prohibited hovering flight for design jet temperatures below about 2000° R, indicating that the burner was too small for the burner Mach number and temperature ratio. When the burner area was increased to 60 percent of the blade-section area, momentum pressure losses were reduced and hovering time became nearly independent of design jet temperature for a wider range of temperatures, except as affected by duct friction losses. A further increase in the burner area to 75 percent of the section area had little effect on flight performance.

Blade-duct area. - Hovering time and flight range are plotted against design jet temperature in figure 14 for the previously shown duct size of 30 percent of the blade-section area and for a larger duct of 50 percent of the section area. The burner area in each case was 75 percent of the blade-section area and the pressure ratio was 2.5. Improvements in hovering time and flight range given by the 50-percent duct over the 30-percent duct were principally due to decreased duct friction pressure losses. A further increase in the duct area provided only a slight improvement in flight performance at a pressure ratio of 2.5.

Combined effects of increased burner and duct areas. - In the preceding sections, it was shown that flight performance at low design jet temperatures and a pressure ratio of 2.5 is significantly improved when burner areas are increased from 45 to 75 percent of the section area and blade-duct areas are increased from 30 to 50 percent of the section area. Similar performance improvements can be realized, of course, for other pressure ratios. Figure 15 gives hovering time and range as functions of design jet temperature for pressure ratios of 2.25 and 3.0 when the 75-percent burner and 50-percent duct were employed; for comparison, flight performance for a pressure ratio of 2.5 has been replotted from figure 14. Hovering time is now maximum (5.55 hr) for a pressure

ratio of 2.5 and is nearly independent of design jet temperature over a wide range. Forward flight range is maximum (765 nautical miles) for a pressure ratio of 2.5 and a jet temperature of 3500° R, a value slightly higher than the design temperature limit. A design jet temperature of 3000° R, however, gives nearly equal range while providing the required reserve power. Comparison of the flight performance results given in figures 11 and 15 emphasizes that the performance benefits resulting from the use of large burners and ducts are greatest for engine operating conditions where high duct Mach numbers are required, that is, at low design jet temperatures and low design pressure ratios.

Rotor tip speed. - Because constant thrust coefficient and constant solidity were assumed for the rotors of this investigation, blade chord and blade-section area decrease with increasing design tip speed; the physical areas that are represented by the ratios of duct area to section area and the ratios of burner area to section area also decrease. System pressure losses are therefore higher at the higher tip speeds. The effects of changes in tip speed on flight performance are illustrated in figure 16. For these calculations, a pressure ratio of 3.0, a design jet temperature of 3000° R, a duct area of 30 percent, and a burner area of 45 percent of the blade-section area were used. In addition to the system pressure loss, two other factors influence the trend of flight performance with changing tip speed: (1) Increased tip speeds improve the propulsive efficiency of the tip jets; and (2) increased tip speeds, at constant C_T, raise the profile and induced-drag power requirements of the helicopter rotor. In the tip-speed range from 500 to 700 feet per second, the flatness of the curves in figure 16 indicates that these counteracting effects have nearly cancelled and flight performance is relatively independent of tip speed. Between 700 and 900 feet per second, increased rotor drag and increased duct losses overbalance the gain in propulsive efficiency and flight performance suffers. Inasmuch as compressible-drag divergence was not included in the rotor drag calculations, the curves are dashed above 700 feet per second to indicate that the flight performance results are optimistic in this range.

Variable- and fixed-area tip-jet nozzle operation. - Hovering time and flight range are plotted in figure 17 for a power-plant configuration in which the tip-nozzle area is fixed. For comparison, the flight performance is also given for the variable-area configuration with corresponding power-plant variables (P_3/P_2, 3.0; duct area, 30 percent; burner area, 45 percent). No attempt was made to optimize the power-plant variables for the fixed-area performance calculation, and off-design operation for this system was carried out as described in appendix A. The superiority in flight performance of the variable-area nozzle configuration is explained by consideration of the thermal and propulsive efficiencies of the pressure jet.

3355

During off-design operation with the fixed-area configuration, pressure ratio and air flow of the auxiliary compressor are progressively reduced. As shown in appendix A, jet temperatures remain nearly constant during this process. On the other hand, with the variable-area configuration, pressure ratio and air flow of the compressor are held at the design values during flight, and jet temperatures are lowered by decreasing the fuel flow to the tip burners. Comparison of the two modes of operation indicates that, for a given rotor power, more tip-burner fuel is required for the fixed-area configuration as flight progresses because pressure and air flow have been reduced. The result of this heat addition at a lower pressure is decreased thermal efficiency. Similarly, propulsive efficiency for the variable-area configuration progressively improves during flight while remaining nearly constant for the fixed-area configuration. Approximate initial and final values for thermal, propulsive, and over-all efficiencies are compared for the two nozzle configurations in the following table:

	Variable area		Fixed area	
	Initial	Final	Initial	Final
Thermal efficiency, percent	18.0	14.0	18.0	10.0
Propulsive efficiency, percent	41.0	59.0	41.0	48.0
Over-all efficiency, percent	7.4	8.3	7.4	4.8

This comparison of power-plant efficiencies shows a rise in over-all efficiency during flight for the variable-area configuration and a reduction in over-all efficiency for the fixed-area case. The superiority in over-all efficiency is reflected in the superiority in hovering duration and range of the variable-area configuration.

Engine specific weight and auxiliary-compressor efficiency. - Flight performance results presented in figures 11 to 17 were based on an assumed power-plant specific weight of 0.65 pound per shaft horsepower for the gas turbine plus the auxiliary compressor. Depending upon the power-plant design parameters, total power-plant weights were between 4 and 8 percent of the helicopter gross weight. In order to reveal the sensitivity of helicopter flight performance to engine weight, the power-plant specific weight was arbitrarily increased from 0.65 to 1.0 pound per shaft horsepower and calculations similar to those plotted in figure 11 were repeated. These calculations showed that hovering time was reduced about 7 percent for a 54-percent increase in engine weight.

In order to reveal the sensitivity of helicopter flight performance to changes in auxiliary-compressor efficiency, the design-point efficiency for the compressor was reduced from 0.87 to 0.84 and flight-performance calculations were repeated. At a design jet temperature of 3000° R and a pressure ratio of 3.0, this reduction in the design-point efficiency reduced the hovering time approximately 2.5 percent.

Effects of Helicopter Design Parameters on Flight Performance

Pay load. - The preceding discussion on the effects of power-plant design parameters on flight performance was given for the helicopter with a fuel load equal to its total disposable load. For a helicopter with a fixed gross weight, pay load is accommodated only at the expense of fuel load. Hovering duration and flight range for the pressure-jet helicopter designed for maximum duration and range are given as functions of pay load in figure 18. With this helicopter, pay loads of nearly 50 percent of the gross weight can be carried for missions of extremely short duration. For short-range load-lifting missions, use of a lower-pressure-ratio pressure-jet system will provide more thrust per pound of power-plant weight at the expense of specific fuel consumption, allowing, therefore, somewhat heavier pay loads. Unless the rotor is specifically designed as a low-speed load lifter, however, these improvements in pay-load capacity are very small, amounting to less than a 0.5-percent increase in pay load for the present configuration. Furthermore, selection of the power plant strictly on the basis of high-pay-load, short-range mission requirements will significantly decrease maximum hovering or range capabilities as discussed in previous sections. Therefore, regardless of the design mission of the pressure-jet helicopter, the power plant should be designed to give maximum possible hovering duration and flight range. With this power plant, performance is maximum for missions of long duration and is very nearly maximum for short-range, high-pay-load missions.

Gross weight. - For a rotor in which disk loading, solidity, and number of blades are held constant, changes in helicopter gross weight will have no significant effect on the choice of the optimum power plant, inasmuch as pressure-jet air flow, horsepower, blade-duct areas, and other power-plant parameters are all directly proportional to gross weight. For helicopters of other gross weights, however, values for the rotor parameters different from those assumed herein may be desirable. These possible variations in the principal rotor parameters that accompany a change in gross weight can affect the choice of optimum power plant in the manner subsequently discussed.

Rotor geometry. - An increase in the number of rotor blades will, for constant solidity, generally decrease the duct area available for a given air flow. The resulting increase in duct Mach number places added emphasis on the higher compressor pressure ratios and jet temperatures with possible decrease in performance. Similarly, for constant rotor solidity, an increase in disk loading will generally decrease the blade-duct area because of reduced blade chord and increase the duct Mach number. Because the external rotor aerodynamics are affected in this case, duct Mach number is further increased by the required higher air flow. In consideration of power-plant performance, therefore, it is desirable to select a rotor with a minimum practical number of blades

3355

CQ-3

and minimum disk loading. On the other hand, an increase in rotor so-
lidity will increase the duct area available for a given air flow, and
high solidities are therefore desirable for best power-plant perform-
ance. In all cases, selection of design values for the pressure-jet
helicopter rotor will be governed by consideration of both power-plant
performance and rotor performance. Detailed examination of these inter-
acting effects and explicit investigation of the effects of gross weight
are beyond the scope of this analysis.

SUMMARY OF RESULTS

The performance of a pressure-jet power plant for a helicopter was
computed for a wide range of compressor pressure ratios and jet temper-
atures. The effects of rotor tip speed and burner and duct areas were
also investigated.

For all pressure ratios, the higher jet temperatures gave higher
specific thrusts, with maximum tip-jet thrusts being developed at the
stoichiometric temperature limit of 4000° R. In general, rotor horse-
power increased about 60 percent when the jet temperature was raised
from 2000° to 4000° R for a given pressure ratio and tip speed. On the
other hand, thrust specific fuel consumption of the tip burner plus gas
turbine was about 35 percent higher at a jet temperature of 4000° than
at 2000° R. The minimum thrust specific fuel consumption and the cor-
responding jet temperature were functions of the auxiliary-compressor
pressure ratio.

Inasmuch as there was no unique combination of compressor pressure
ratio and jet temperature which would give both maximum thrust and mini-
mum specific fuel consumption, the integrated performance of several
power-plant - helicopter combinations was calculated. It was found from
these calculations that helicopter performance in hovering and forward
flight was relatively insensitive to changes in the principal power-
plant variables over a considerable range. For example, hovering time
within 10 percent of the maximum was obtained for a range of pressure
ratios from 2.5 to 4.0 and jet temperatures from 2500° to 4000° R.

When blade-duct and tip-burner areas were increased, the usable
range of power-plant variables was expanded to lower pressure ratios
and lower jet temperatures. For example, if burner and duct areas
were increased 67 percent above the conservative values that were in-
itially assumed, hovering times within 10 percent of the maximum were
obtained with jet temperatures and pressure ratios as low as 1750° R
and 2.25, respectively.

For the range of rotor tip speeds from 500 to 700 feet per second, hovering time and flight range were nearly constant. At 900 feet per second, even without allowance for rotor compressible drag divergence, hovering time and flight range were 15 to 20 percent lower than at a tip speed of 700 feet per second.

For the major part of this investigation, variable-area operation of the tip-jet nozzle was assumed. To provide an indication of the effects of nozzle configuration, performance was calculated for a single pressure-jet power plant with a fixed-area tip-jet nozzle. Although the power-plant variables were not optimized for the fixed-area system, the 30-percent reduction in hovering time and flight range that was calculated for this configuration gave evidence of the inherent superiority of the variable-area mode of operation.

Lewis Flight Propulsion Laboratory
    National Advisory Committee for Aeronautics
        Cleveland, Ohio, December 21, 1954

APPENDIX A

PERFORMANCE OF PRESSURE-JET POWER PLANT

Cycle Calculations

Torque equilibrium of the jet-driven helicopter rotor is established when the rotor-blade total drag force is balanced by the net propulsive thrust of the tip-jet units. The net thrust of the pressure jet is equal to the jet thrust minus the force required to pump the air and fuel from the hub to the blade tips. An outline of the calculations giving net thrust per pound of air flow as a function of net thrust per unit duct area follows. Subscript numbers refer to station numbers in the pressure-jet system and are identified in figure 1; symbols are defined in appendix C.

The net thrust F_n of the pressure jet is given by the expression

$$F_n = F_j - F_p \tag{A1}$$

The equivalent pumping force F_p for air and fuel in the blades is

$$F_p = \frac{W_a}{g}(1 + f/a)V_t \tag{A2}$$

The jet thrust F_j was found from the expression

$$F_j = \frac{W_a}{g}k_2\sqrt{T_6}(1 + f/a)C_{v,j} \tag{A3}$$

where k_2 is a function of the jet pressure ratio P_6/p_0 and the ratio of specific heats γ (assumed to be 1.34 for the jet).

The jet pressure ratio P_6/p_0 was determined by tracing the total pressure through the system beginning at the inlet of the auxiliary compressor. At this point, the ram-pressure rise was neglected so that the total pressure at the diffuser inlet P_1 was taken equal to the ambient pressure p_0, or

$$P_1 = p_0 \tag{A4}$$

The diffuser loss was assumed constant and therefore

$$\frac{P_2}{P_0} = 0.95 \tag{A5}$$

The discharge pressure of the compressor P_3 was raised above that at the compressor face P_2 by the assumed compressor pressure ratio, or

$$P_3 = P_2 \left(\frac{P_3}{P_2} \right) \tag{A6}$$

The pressure P_4 was equal to that at the compressor outlet P_3, minus the friction loss $k_f q_x$, plus the pressure rise due to centrifugal force in the blades $1/2 \rho_x V_t^2$, or

$$P_4 = P_3 - 1/2 \rho_x \left(V_x^2 k_f - V_t^2 \right) \tag{A7}$$

where the density ρ_x and the air velocity V_x in the duct were computed from the temperature and pressure at the compressor discharge for a series of assumed values for the duct Mach number M_x. The friction pressure factor k_f was assumed to equal 2.5 and includes the individual contributions of the fuselage ducts, blade ducts, elbows, and combustor flameholders. Calculation of the blade-duct losses using friction coefficients based on the duct Reynolds number indicated that this estimate of system pressure loss is conservative.

The momentum pressure loss in the burner was computed for the calculated M_5 and total-temperature ratio T_6/T_3. The jet pressure was found from

$$P_6 = P_4 \, f(M_5, \, T_6/T_3) \tag{A8}$$

Temperature throughout the pressure-jet system was found in the following manner:

(1) Total temperature was assumed constant through the inlet diffuser, or

$$T_0 = T_1 = T_2 \tag{A9}$$

(2) The temperature rise in the compressor was calculated from

$$\frac{T_3}{T_2} = \frac{\left(\frac{P_3}{P_2} \right)^{0.2754} - 1}{\eta_c} + 1 \tag{A10}$$

For the cycle calculations that give the power-available curves, the auxiliary-compressor efficiency η_c was assumed constant at 0.87.

(3) Heat losses from the duct air through the duct walls were assumed to balance the energy increase due to centrifugal compression so that $T_4 = T_3$.

(4) The temperature ratio T_6/T_3 was computed from the compressor-outlet temperature T_3 and the assumed jet temperature T_6.

From equations (A1), (A2), and (A3) and the value of f/a from reference 8, expressions giving the net thrust per pound of air and the net thrust per unit duct area were derived as follows:

$$\frac{F_n}{W_a} = \left(\frac{F_j}{W_a(1 + f/a)} - \frac{V_t}{g}\right)(1 + f/a) \qquad (A11)$$

and

$$\frac{F_n}{A_x} = \frac{F_n}{W_a} \rho_x V_x \qquad (A12)$$

Because the pressure ratio across the jet nozzle was always greater than critical, the following relation between the duct area A_x and the tip-jet-nozzle area A_6 held:

$$\frac{A_x}{A_6} = \frac{0.5741}{(1 + f/a)} \frac{P_6/P_3}{\sqrt{T_6/T_3}} \qquad (A13)$$

Off-Design Operation of Pressure Jet

Variable-area jet nozzle. - In off-design operation with a variable-area jet nozzle, the auxiliary compressor is held at design values of speed, pressure ratio, and air flow, while the fuel flow to the tip burners and the jet-nozzle area are reduced as the power required decreases. The operation of the pressure-jet system during this power-reduction process is illustrated by the operating line AB in figure 5(h). Point A gives the relation between the thrust per pound of air and the thrust per unit duct area at the design hovering condition ($P_3/P_2 = 2.5$; $T_{6,d} = 3500°$ R). As the pressure-jet power is reduced, the system operating point moves along the constant duct Mach number line AB. At point B, the jet temperature has decreased to the compressor-outlet temperature (cold-jet condition) and the fuel flow to the tip burners has been entirely cut off. Further reductions in pressure-jet power are obtained, if necessary, by operating the compressor at design speed but at a reduced pressure ratio, obtained in this case by an increase in the tip-nozzle area.

Fixed-area jet nozzle. - In off-design operation with a fixed-area
jet nozzle, the speed, pressure ratio, and air flow of the auxiliary
compressor are reduced and the fuel flow to the tip burners is de-
creased. This process is illustrated by reference to the power-
available chart in figure 5(q). The assumed ratio of the nozzle area
to the duct area A_6/A_x in this plot is 0.6. Similar charts were con-
structed for an appropriate range of tip-nozzle areas.

The operating line of the auxiliary compressor (fig. 4) has been
superimposed on the map of figure 5(q) so as to pass through the de-
sign pressure ratio and the required initial hovering rotor tip thrust
(point C). Throughout a given helicopter flight, the operating point
of the fixed-nozzle pressure-jet system is found at the intersection
of the compressor operating line and the appropriate thrust line. As
the required tip thrust decreases, the operating point of the system
moves along the line CD, intersecting successively lower thrust-required
values. Because of the character of the selected compressor operating
line, the operating line for the fixed-nozzle-area pressure jet almost
coincides with a constant-jet-temperature line. Consequently, the as-
sumed fixed-area off-design operation of the pressure jet approximates
constant-jet-temperature operation.

APPENDIX B

HELICOPTER DESIGN CONSIDERATIONS

Rotor design for efficient operation in both hovering and forward flight represents a compromise. In both flight conditions, optimum performance results when the rotor is operating at mean blade angles near stall (ref. 7). However, stall on the retreating blade usually establishes the limit to forward-flight speed, and a design mean lift coefficient is selected that will give acceptable rotor performance in both hovering and forward flight. In reference 7, the relation between mean lift coefficient $\overline{C}_L$, thrust coefficient C_T, and rotor solidity σ is given as

$$\overline{C}_L = \frac{6C_T}{\sigma} \tag{B1}$$

For the usual range of design thrust coefficients, higher values of the quantity C_T/σ give higher rotor hovering efficiencies while limiting maximum speed in forward flight. A value of C_T/σ equal to 0.07 was used for the rotors considered in this investigation, and equation (B1) gives a value of 0.42 for the design mean lift coefficient.

It was stated previously that a relation exists between tip speed V_t, disk loading w, and rotor solidity σ. Following are the details of this relation:

(1) With an assumed tip speed V_t of 700 feet per second and a disk loading w of 6.0 pounds per square foot, the design thrust coefficient is

$$C_T = \frac{W_g}{\rho_0 \pi R^2 V_t^2} = \frac{w}{\rho_0 V_t^2} = 0.0051 \tag{B2}$$

(2) From this design value for C_T, which was held constant for all rotors in this investigation, and the design $\overline{C}_L$ of 0.42, a rotor solidity of 0.073 is computed from equation (B1).

(3) By using the above constant values of thrust coefficient and solidity, the relation between tip speed, rotor radius, chord, and disk loading is calculated from the equations for C_T and σ.

Rotor Performance Analysis

The blade-element method of rotor analysis was employed in this investigation (ref. 7). In this method, analytical integration of individual element lift and drag contributions requires a power-series approximation to the airfoil-section profile-drag coefficient c_{d_0}. The usual form of the power series is:

$$c_{d_0} = \delta_0 + \delta_1 \alpha_r + \delta_2 \alpha_r{}^2 \tag{B3}$$

The drag characteristics of low-drag airfoils near stalling angles of attack or at high Mach numbers complicate the task of selecting the power-series constants. However, it is demonstrated in reference 9 that reasonable agreement between the results of the analytical method, using the conventional power series, and experimental rotor results is obtained if the operating condition leading to high advancing blade angles of attack combined with near-critical tip Mach numbers is avoided. This condition has therefore been established herein as a limit to the usefulness of rotor performance calculations. Another limit is the usual one requiring that retreating blade angles of attack remain below stalling angles. Section-drag data for the 64_1-012 airfoil (ref. 10) were evaluated for a Mach number calculated at the three-quarter blade-radius point. Constants of the section-drag power series were determined from these data. With the exception of the 900-foot-per-second tip-speed condition, the drag-divergence power requirements do not significantly affect the rotor performance results. Inasmuch as calculated helicopter range and hovering duration at a tip speed of 900 feet per second are inferior to the performance at 700 feet per second, it was not considered worthwhile to refine the rotor calculations to include drag-divergence power.

Rotor Hovering Performance

Rotor performance in hovering flight was calculated by use of equation (B4). While this equation was derived for a rotor with ideally twisted blades, it is demonstrated in reference 7 that the equation can be used for performance calculations for a rotor with linearly twisted blades.

$$C_Q = \frac{C_T{}^{3/2}}{B\sqrt{2}} + \frac{\sigma\delta_0}{8} + \frac{2}{3}\frac{\delta_1}{a}\frac{C_T}{B^2} + \frac{4\delta_2}{\sigma a^2}\left(\frac{C_T}{B^2}\right)^2 \tag{B4}$$

Typical hovering performance results, plotted as thrust coefficient against torque coefficient for a tip speed of 700 feet per second, are given in figure 19(a).

Rotor Forward-Flight Performance

Rotor performance in forward flight was obtained by the method of reference 11. Calculations of the blade angle of attack on the retreating tip were carried through for all flight conditions to provide a check against serious rotor stall. Spot calculations for the angle of attack on the advancing tip were made for the higher tip-speed ratios to ensure that high blade angles did not occur in combination with near-critical tip Mach numbers.

A convenient presentation of the results of the forward-flight rotor calculations is one in which the thrust coefficient C_T is plotted against the torque coefficient C_Q for fixed values of the useful drag-lift parameter $(D/L)_u$. One such plot was obtained for each value of the tip-speed ratio μ. The entire calculation was repeated for each value of the rotor tip speed V_t. A typical forward-flight rotor performance plot is shown in figure 19(b).

The useful drag-lift ratio $(D/L)_u$ is a measure of the useful component of rotor thrust in the forward-flight direction. In steady forward flight, this component balances the fuselage drag force, which is fixed for any given flight velocity. During a given flight plan, the $(D/L)_u$ parameter was calculated and used with the rotor performance charts to provide the helicopter power requirements.

Helicopter Component Weights

Component weights assumed for this investigation are listed in the following table and are considered to be representative for a helicopter of 30,000 pounds gross weight:

	Tip speed, ft/sec			
	500	600	700	900
Disk loading, lb/sq ft	3.05	4.4	6.0	9.9
Rotor radius, ft	56.0	46.7	40.0	31.1
Weight of components, lb				
Rotor blades	3,315	3,080	2,880	2475
Hub	2,815	2,605	2,425	2185
Tail surfaces	180	180	180	180
Fuselage	2,600	2,295	2,055	1730
Landing gear				
Controls				
Instruments				
Hydraulic and electrical systems	3,242	3,242	3,242	3242
Communications equipment				
Furnishings				
Total weight, lb	12,152	11,402	10,782	9812
Ratio of structure to gross weight	0.405	0.380	0.360	0.327

CQ-4

APPENDIX C

SYMBOLS

The following symbols are used in this report:

A   area, sq ft

a   slope of curve of section lift coefficient against section
                angle of attack, per radian

B   tip loss factor

b   number of blades per rotor

$\overline{C}_L$ rotor mean lift coefficient

C_Q rotor torque coefficient

C_T rotor thrust coefficient

$C_{v,j}$ jet-velocity coefficient

c_{d_o} section profile-drag coefficient

$(D/L)_u$ equivalent useful drag-lift parameter

F_j pressure-jet thrust, lb

F_n pressure-jet net thrust, lb

F_p equivalent pumping force, lb

f/a   fuel-air ratio of tip combustors

g   gravitational constant

k_f friction pressure-loss factor

M   Mach number

P   total pressure, lb/sq ft

ΔP_f total-pressure loss due to duct friction, lb/sq ft

p   static pressure, lb/sq ft

q   dynamic pressure, lb/sq ft

R   rotor radius, ft

T   rotor thrust, lb

T_i total temperature, power-plant stations   i = 0 to 6, °R

V   velocity, ft/sec

W_a air flow through auxiliary compressor, lb/sec

W_g helicopter gross weight, lb

w   rotor disk loading, lb/sq ft

α_r blade-element angle of attack, radians

γ ratio of specific heats

$\delta_0, \delta_1, \delta_2$ coefficients in three-term drag polar

η_c auxiliary-compressor efficiency

μ tip-speed ratio

ρ mass density of air, slugs/cu ft

σ rotor solidity

Subscripts:

d   design point

p   parasite-drag flat plate

t   rotor tip

x   blade duct

0   free stream

1   diffuser inlet

2   auxiliary-compressor inlet

3   auxiliary-compressor discharge

4   tip end of constant-area blade duct

5   tip combustor inlet

6   tip-jet nozzle

REFERENCES

1. Katzenberger, E. F., and Nozick, H. J.: The Selection and Evaluation
     of Powerplants for Helicopters. Paper presented at SAE meeting,
     Detroit (Mich.), Jan. 12-16, 1953.

2. Stuart, Joseph, III.: Comparison of Helicopter Rotor Propulsion
     Systems. Proc. Eighth Annual Forum, Am. Helicopter Soc., Wash-
     ington (D.C.), May 15-17, 1952, pp. 129-146.

3. Falconer, R. W.: The Application of Jet Propulsion to Helicopters.
     Aero. Eng. Rev., vol. 11, no. 9, Sept. 1952, pp. 46-51.

4. Pinkel, Benjamin, and Karp, Irving M.: A Thermodynamic Study of the
     Turbine-Propeller Engine. NACA Rep. 1114, 1953. (Supersedes NACA
     TN 2653.)

5. Radin, Edward J., and Carpenter, Paul J.: Comparison of the Perform-
     ance of a Helicopter Ram-Jet Type Engine under Various Centrifugal
     Loadings. NACA RM L53H18a, 1953.

6. Meyers, G. C., and Heck, A. H.: Charts for Determining the Aerody-
     namic Characteristics of Jet Rotors in Hovering. Rep. No. 1136,
     Helicopter Div., Eng. Dept., McDonnell Aircraft Corp., Apr. 1949.

7. Gessow, A., and Meyers, G. C.: Aerodynamics of the Helicopter. The
     Macmillan Co., 1952.

8. Turner, L. Richard, and Bogart, Donald: Constant-Pressure Combustion
     Charts Including Effects of Diluent Addition. NACA Rep. 937, 1949.
     (Supersedes NACA TN's 1086 and 1655.)

9. Carpenter, Paul J.: Effect of Compressibility on the Performance of
     Two Full-Scale Helicopter Rotors. NACA Rep. 1078, 1952. (Super-
     sedes NACA TN 2277.)

10. Wilson, Homer B., Jr., and Horton, Elmer A.: Aerodynamic Character-
    istics at High and Low Subsonic Mach Numbers of Four NACA 6-Series
    Airfoil Sections at Angles of Attack from -2° to 31°. NACA RM
    L53C20, 1953.

11. Bailey, F. J., Jr.: A Simplified Theoretical Method of Determining
    the Characteristics of a Lifting Rotor in Forward Flight. NACA
    Rep. 716, 1941.

3355
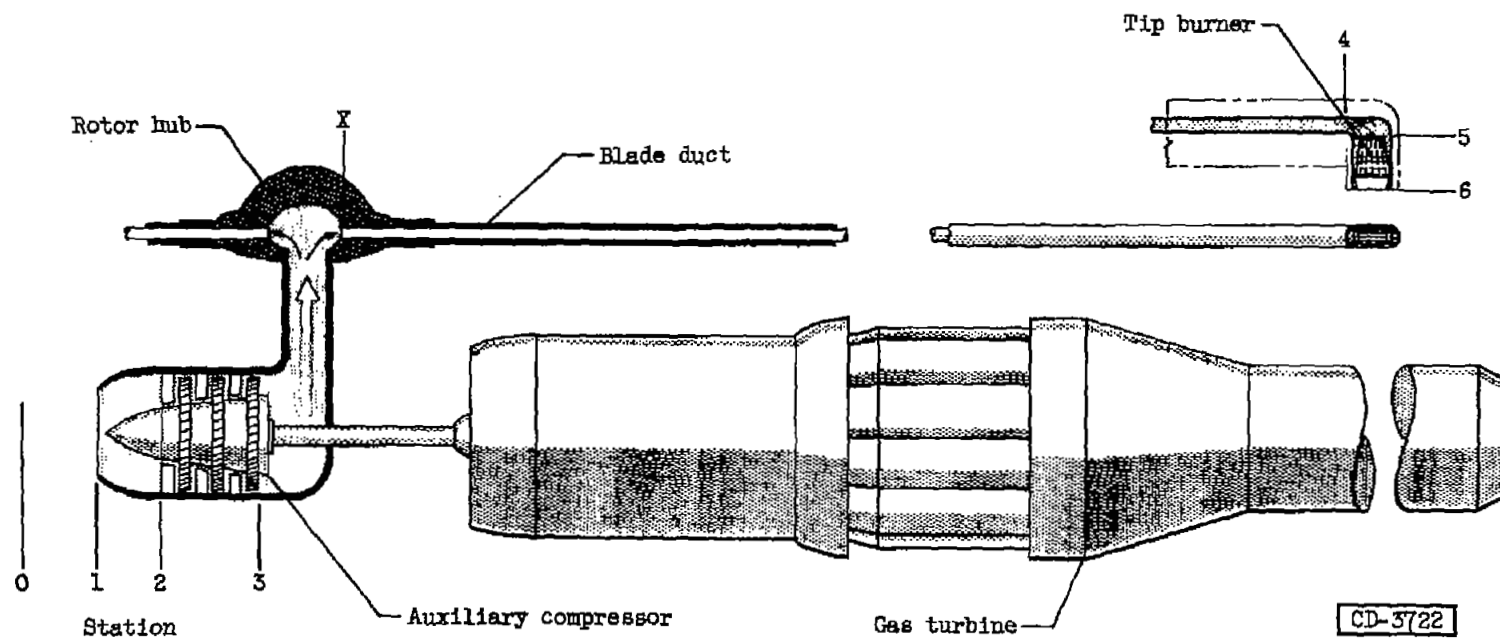
Figure 1. - Schematic of pressure-jet components.
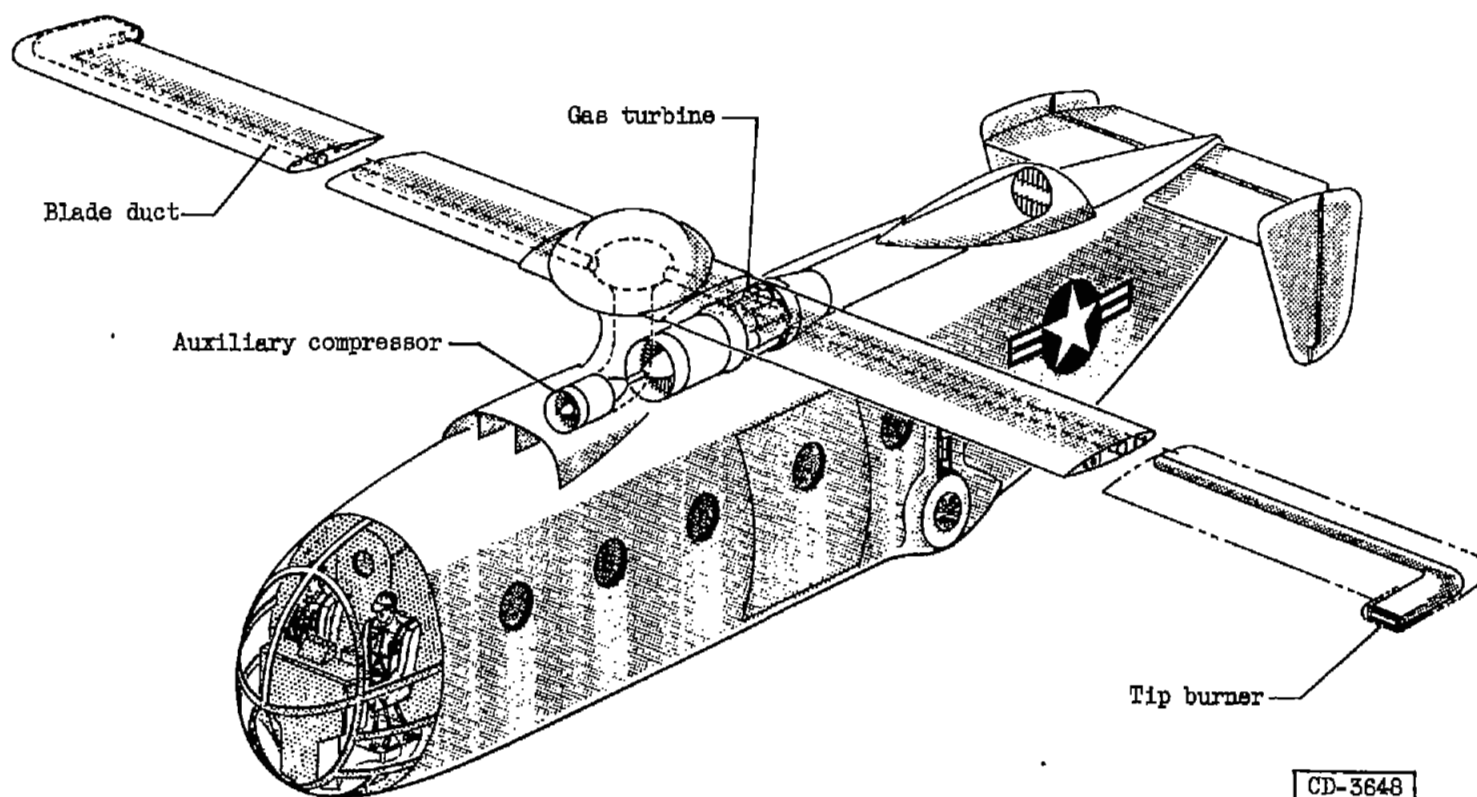
Figure 2. - Assumed configuration for pressure-jet helicopter.
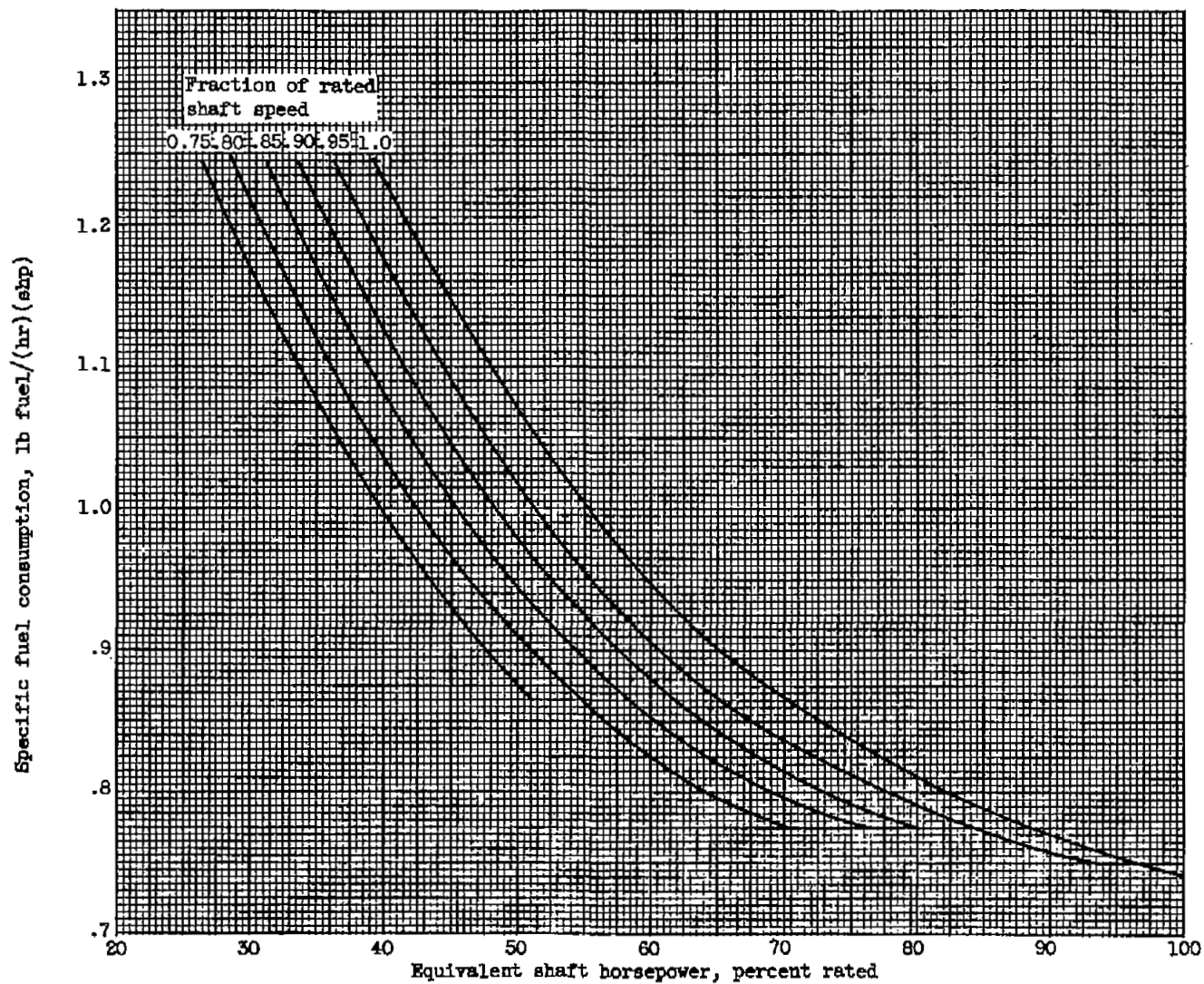
Figure 3. - Specific fuel consumption of gas turbine as function of equivalent shaft horsepower and shaft speed.

3355

CQ-5
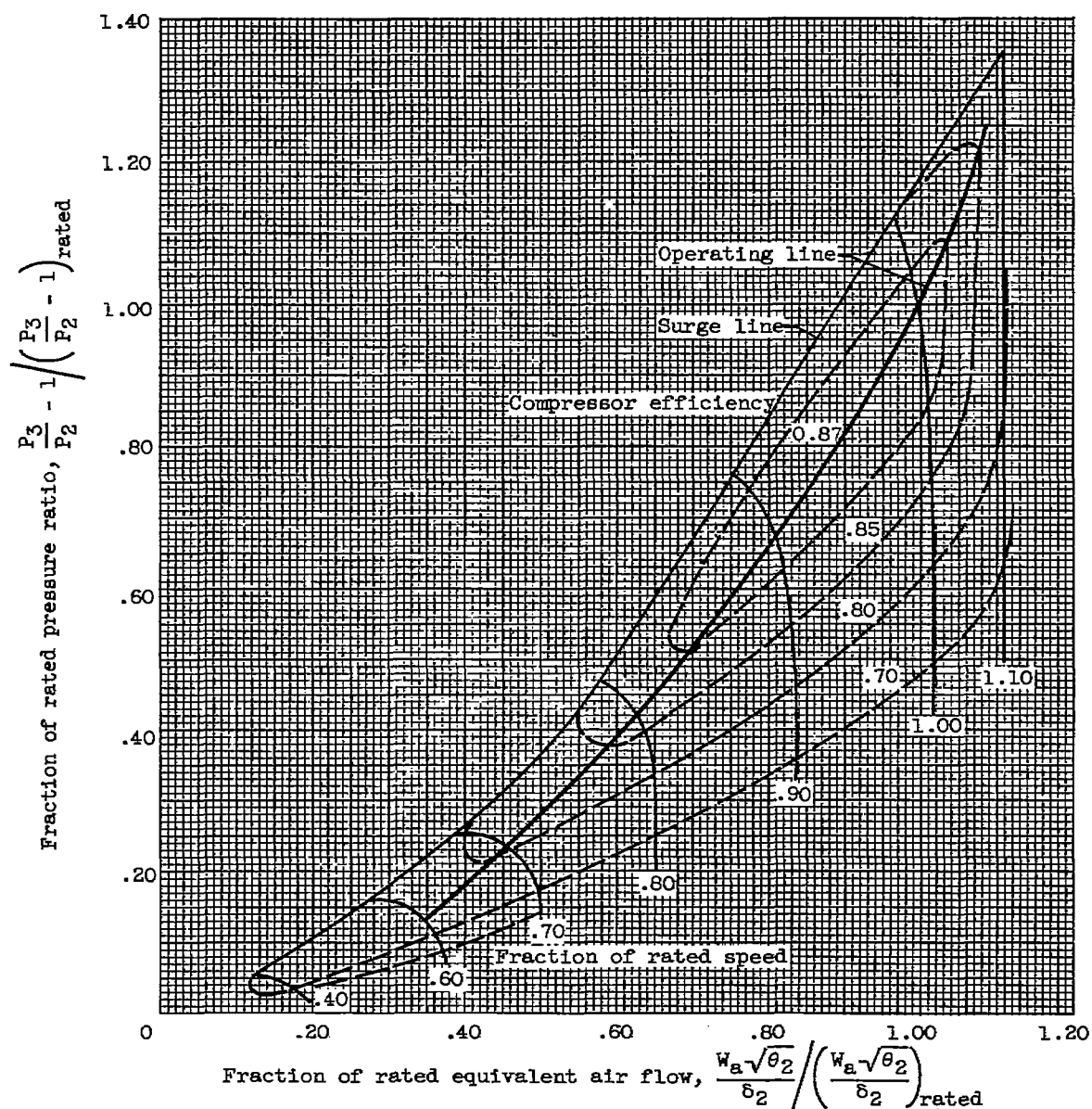
Figure 4. - Performance map for pressure-jet auxiliary compressor.

(a) Variable-area tip-jet nozzle; pressure ratio, 2.5; tip speed, 500 feet per second; $\Delta P_f = 2.5q_x$; burner area/duct area, 1.5.

(b) Variable-area tip-jet nozzle; pressure ratio, 3.0; tip speed, 500 feet per second; $\Delta P_f = 2.5q_x$; burner area/duct area, 1.5.
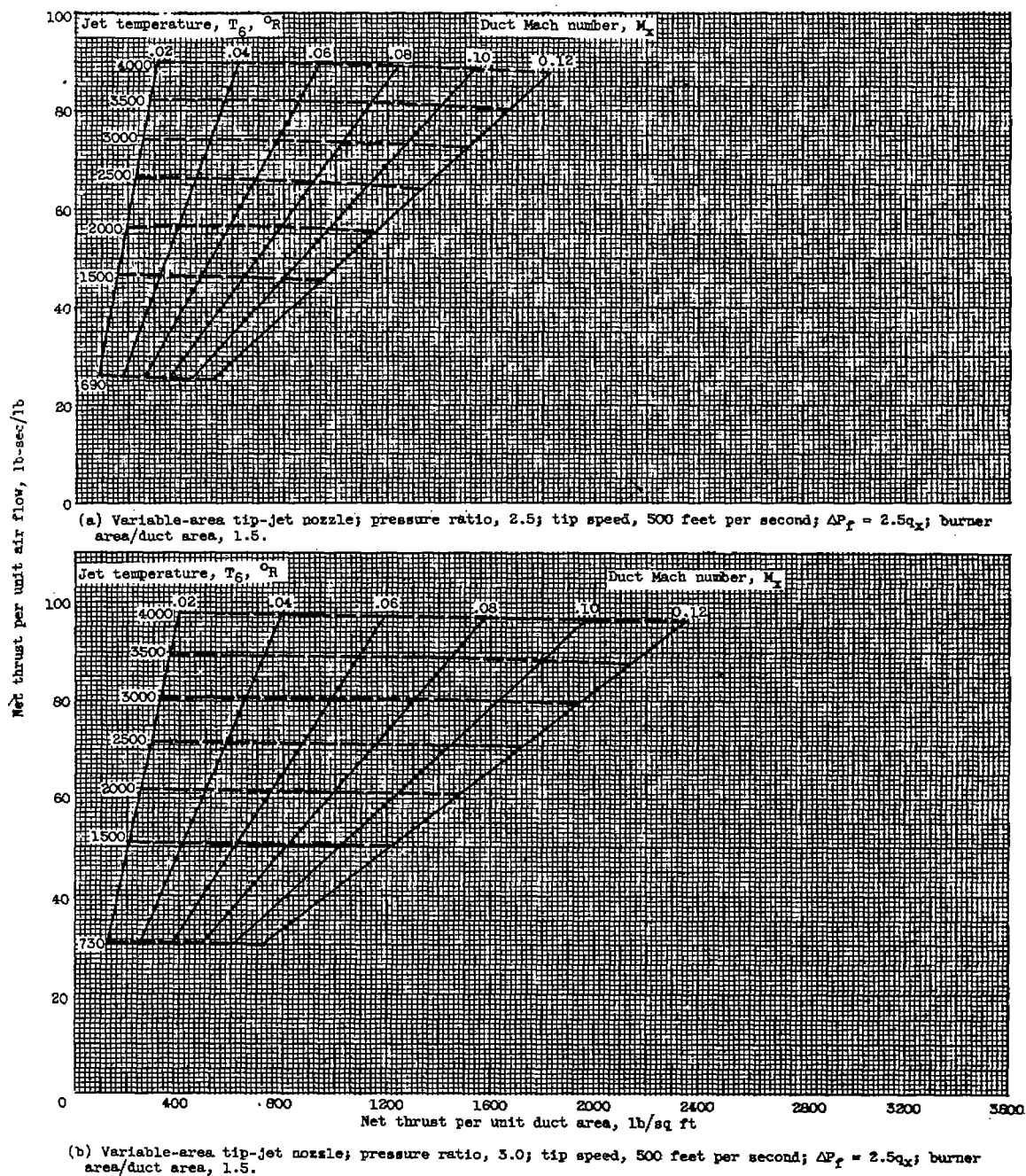
Figure 5. - Power-available chart.

3355

CQ-5 back

(c) Variable-area tip-jet nozzle; pressure ratio, 4.0; tip speed, 500 feet per second; $\Delta P_f = 2.5q_x$; burner area/duct area, 1.5.

(d) Variable-area tip-jet nozzle; pressure ratio, 2.5; tip speed, 600 feet per second; $\Delta P_f = 2.5q_x$; burner area/duct area, 1.5.

Figure 5. - Continued. Power-available chart.

(e) Variable-area tip-jet nozzle; pressure ratio, 3.0; tip speed, 600 feet per second; $\Delta P_f = 2.5q_x$; burner area/duct area, 1.5.
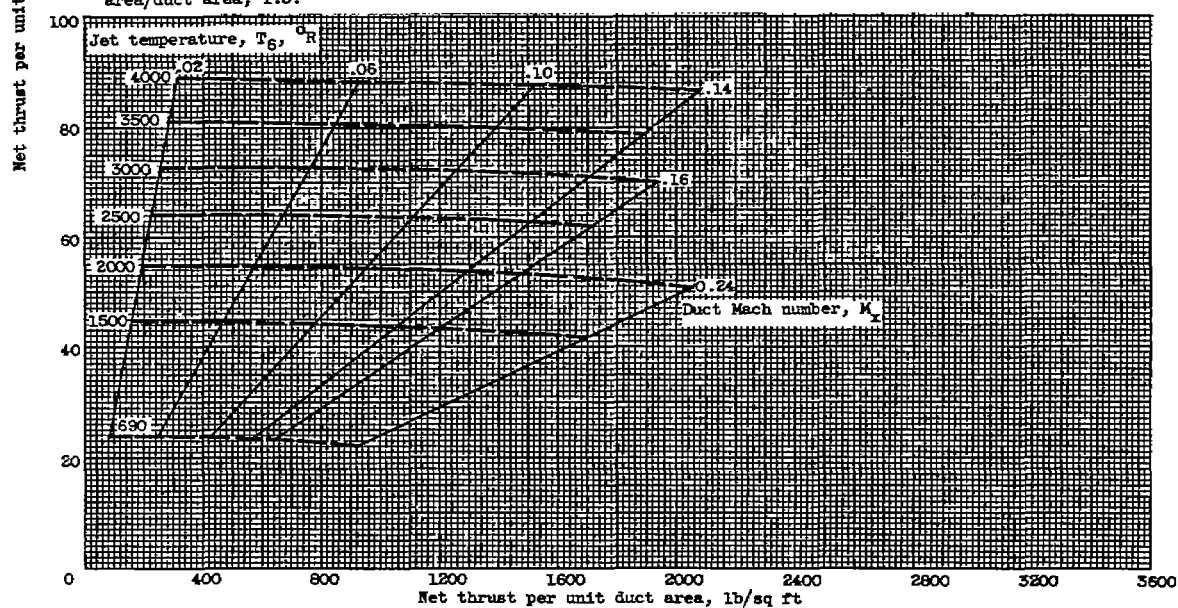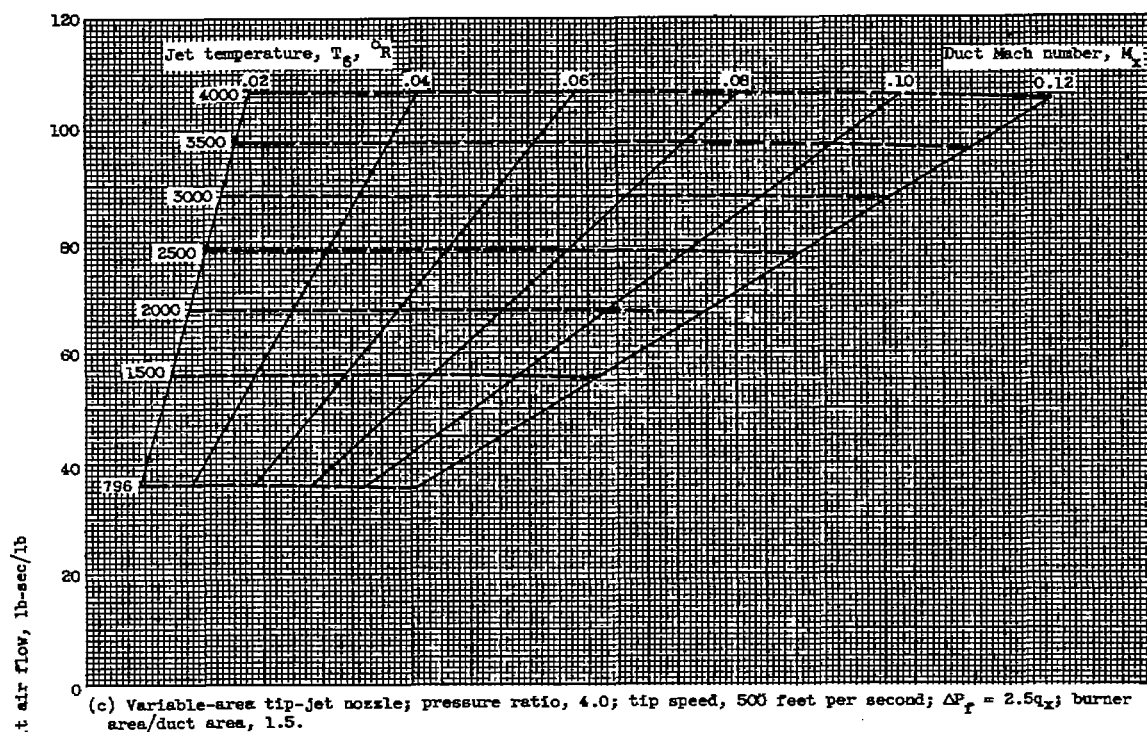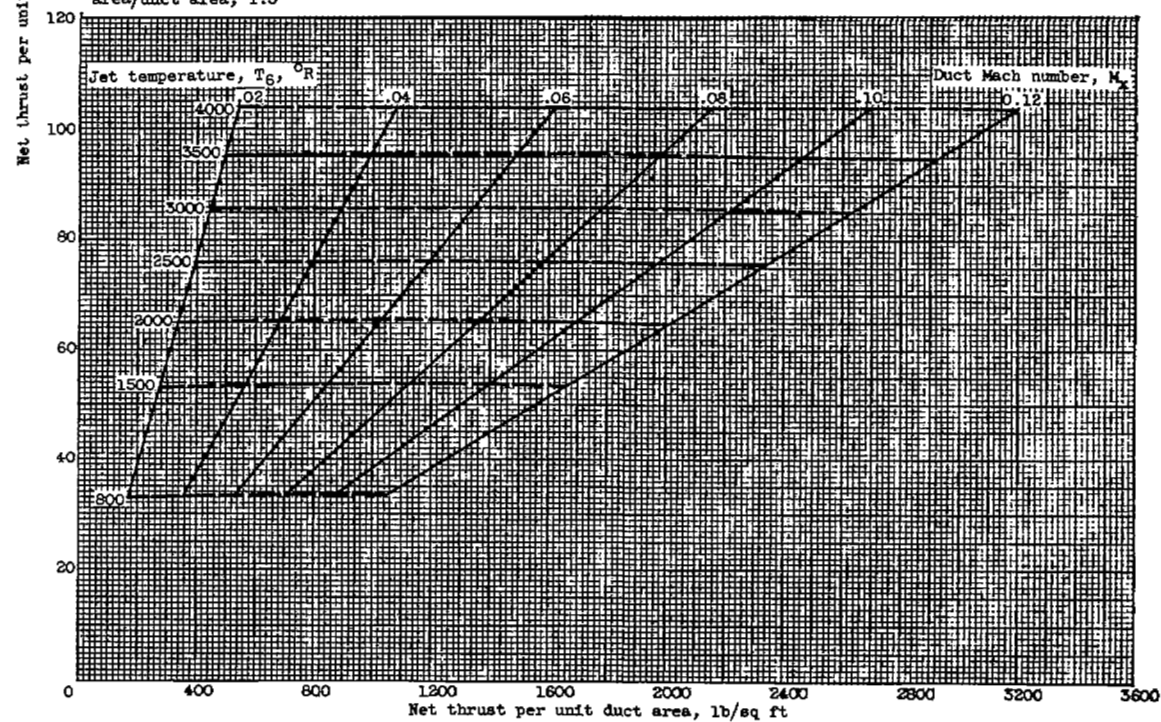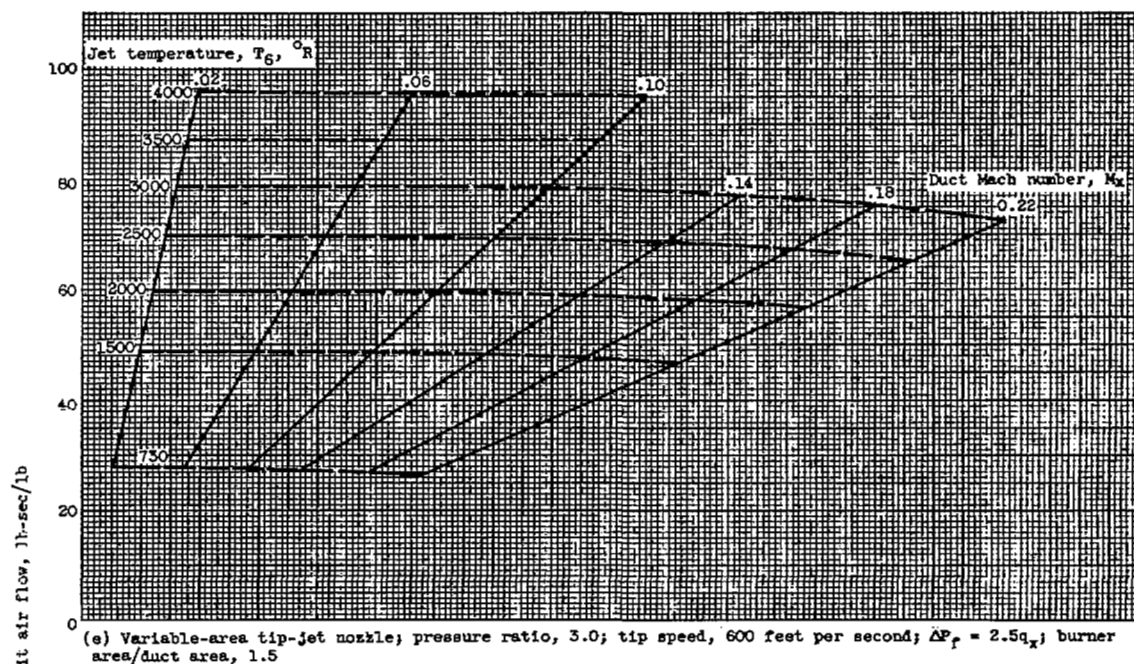
(f) Variable-area tip-jet nozzle; pressure ratio, 4.0; tip speed, 600 feet per second; $\Delta P_f = 2.5q_x$; burner area/duct area, 1.5.

Figure 5. - Continued. Power-available chart.

Net thrust per unit air flow, lb-sec/lb

(g) Variable-area tip-jet nozzle; pressure ratio, 2.25; tip speed, 700 feet per second; $\Delta P_f = 2.5q_x$; burner area/duct area, 1.5.

(h) Variable-area tip-jet nozzle; pressure ratio, 2.5; tip speed, 700 feet per second; $\Delta P_f = 2.5q_x$; burner area/duct area, 1.5.

Net thrust per unit duct area, lb/sq ft
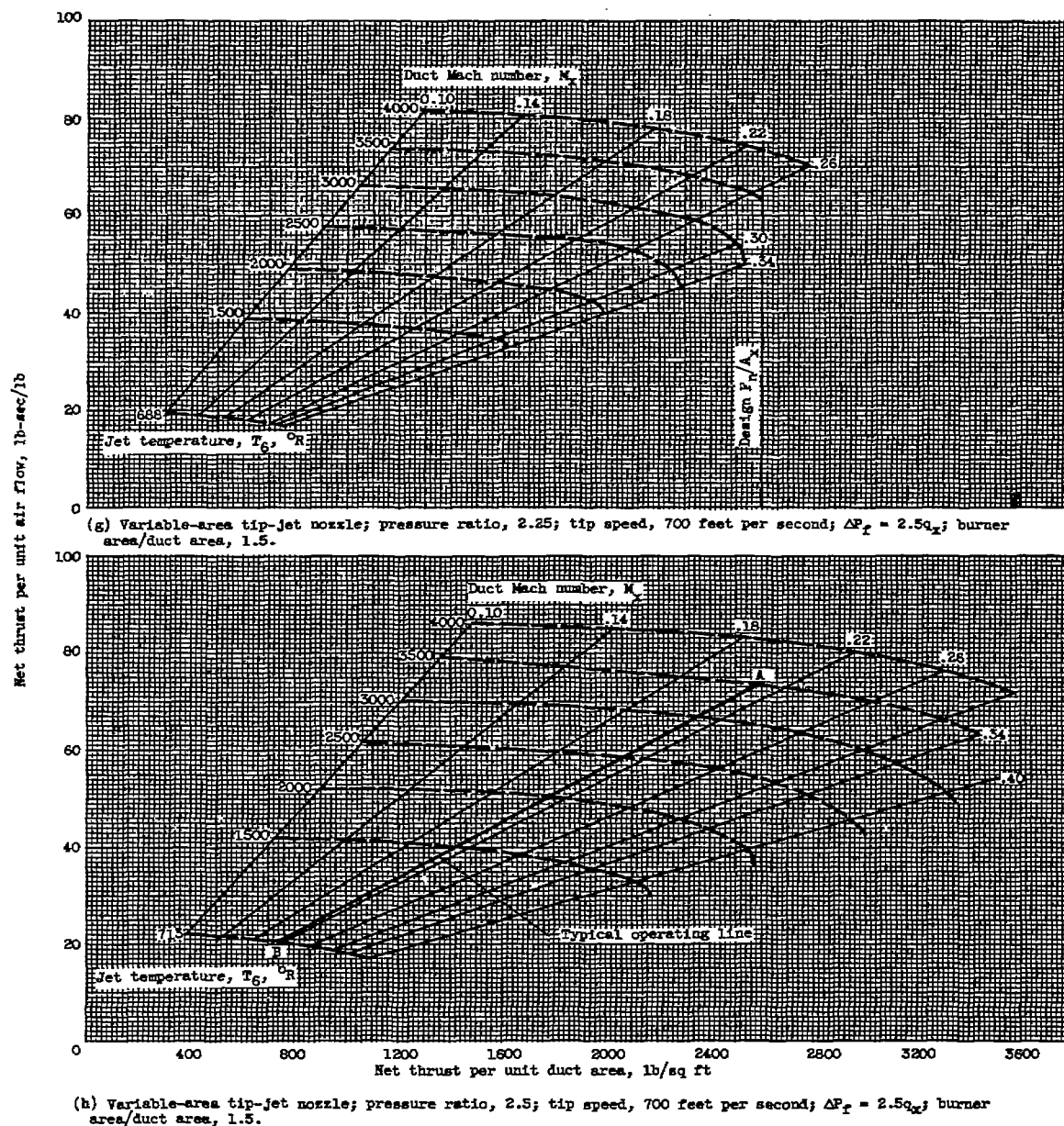
Figure 5. - Continued. Power-available chart.
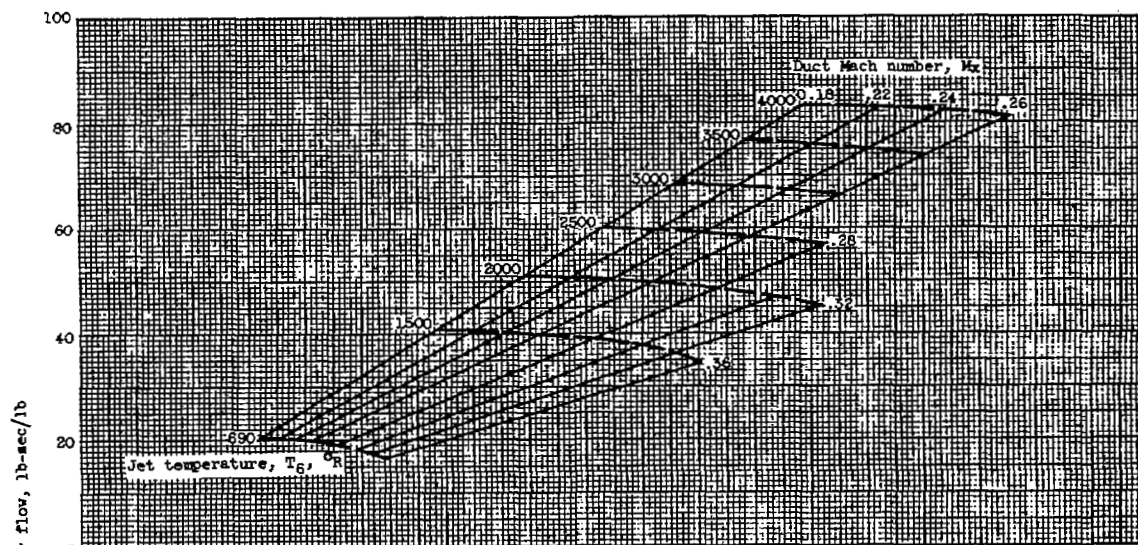
(i) Variable-area tip-jet nozzle; pressure ratio, 2.5; tip speed, 700 feet per second; $\Delta P_f = 2.5q_x$; burner area/duct area, 2.0.
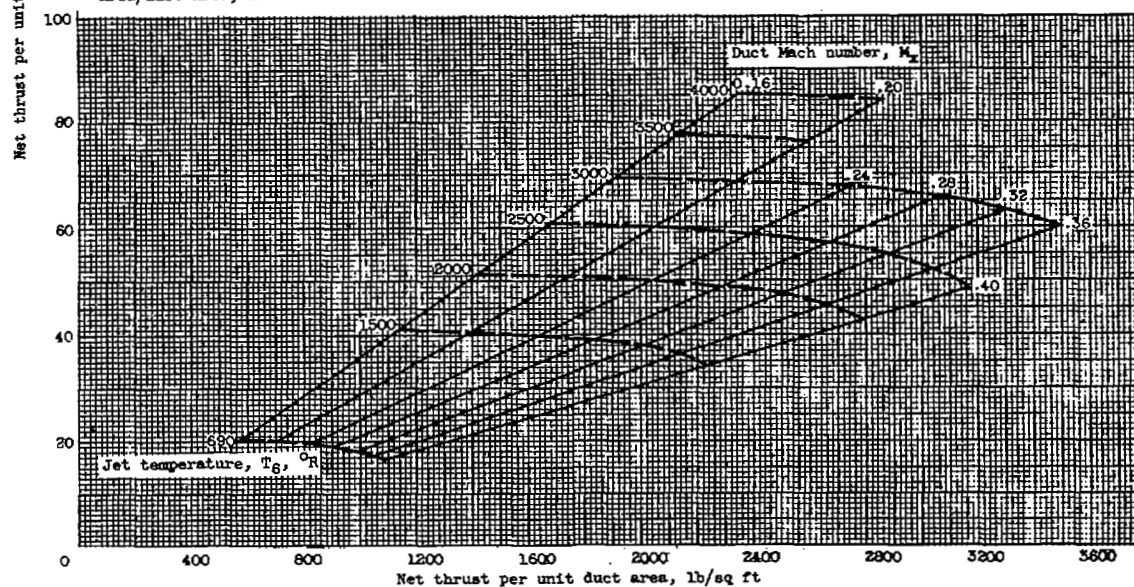
(j) Variable-area tip-jet nozzle; pressure ratio, 2.5; tip speed, 700 feet per second; $\Delta P_f = 2.5q_x$; burner area/duct area, 2.5.

Figure 5. – Continued. Power-available chart.

3355

Net thrust per unit air flow, lb-sec/lb
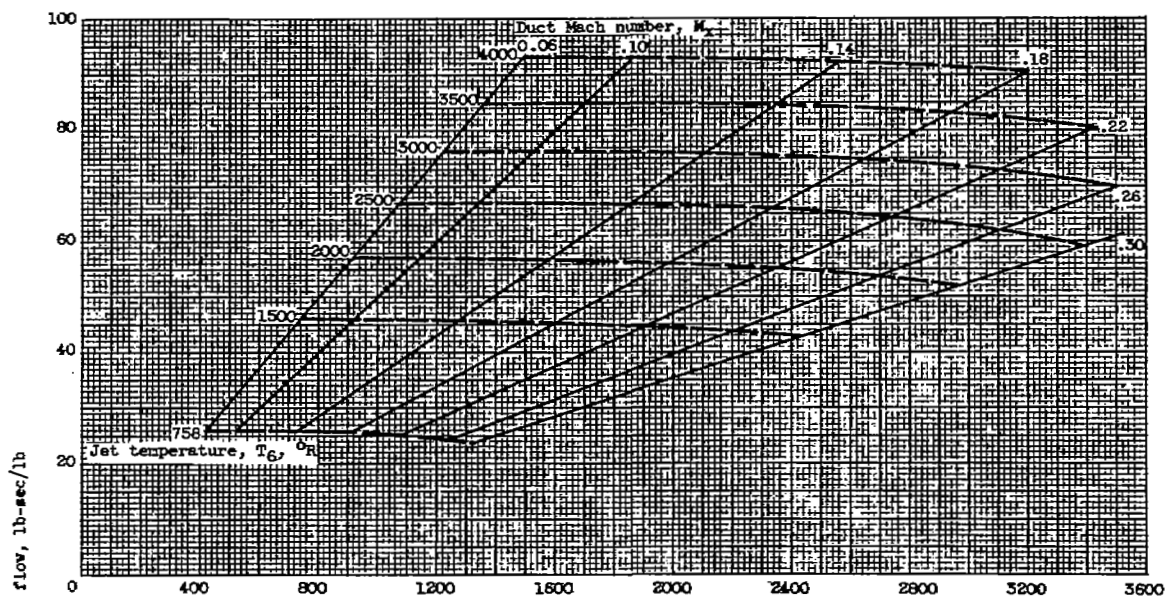
(k) Variable-area tip-jet nozzle; pressure ratio, 3.0; tip speed, 700 feet per second; $\Delta P_f = 2.5q_x$; burner area/duct area, 1.5.
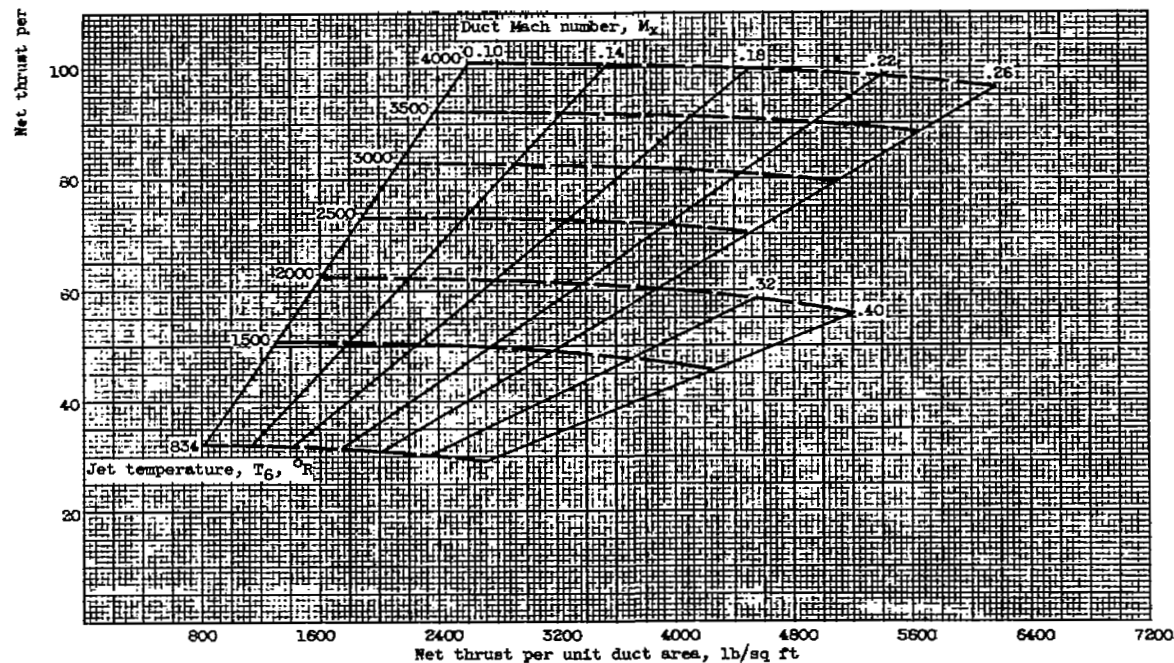
(l) Variable-area tip-jet nozzle; pressure ratio, 4.0; tip speed, 700 feet per second; $\Delta P_f = 2.5q_x$; burner area/duct area, 1.5.

Net thrust per unit duct area, lb/sq ft

Figure 5. - Continued. Power-available chart.
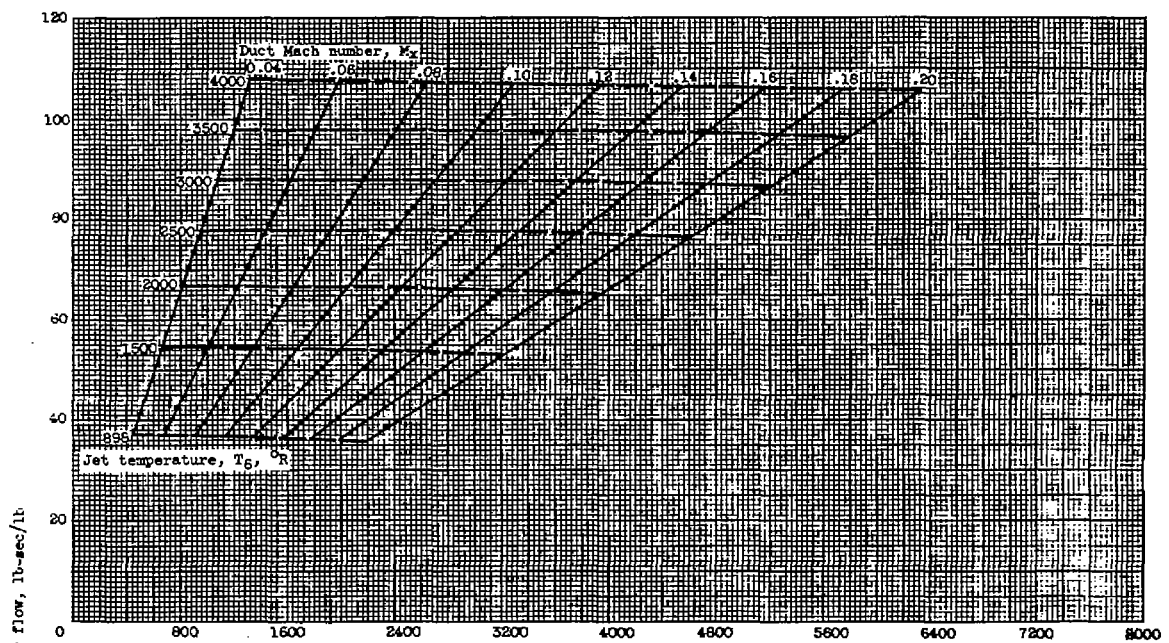
(m) Variable-area tip-jet nozzle; pressure ratio, 5.0; tip speed, 700 feet per second; $\Delta P_f = 2.5q_x$; burner area/duct area, 1.5.
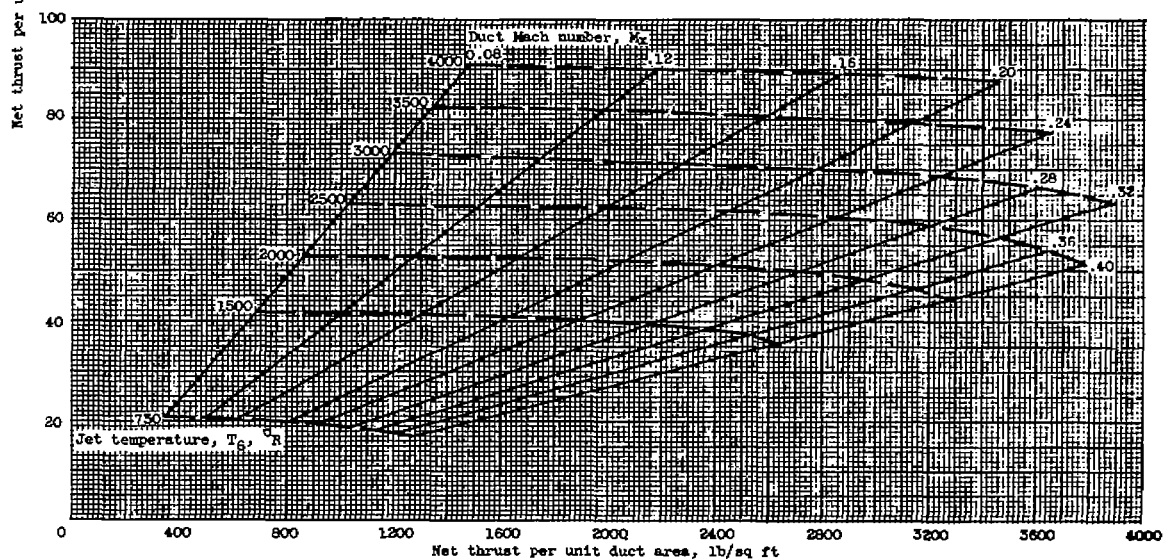
(n) Variable-area tip-jet nozzle; pressure ratio, 5.0; tip speed, 900 feet per second; $\Delta P_f = 2.5q_x$; burner area/duct area, 1.5.

Figure 5. - Continued. Power-available chart.

3355

'CQ-6

Net thrust per unit air flow, lb-sec/lb

(o) Variable-area tip-jet nozzle; pressure ratio, 4.0; tip speed, 900 feet per second; $\Delta P_f = 2.5q_x$; burner area/duct area, 1.5.

(p) Variable-area tip-jet nozzle; pressure ratio, 5.0; tip speed, 900 feet per second; $\Delta P_f = 2.5q_x$; burner area/duct area, 1.5.

Net thrust per unit duct area, lb/sq ft
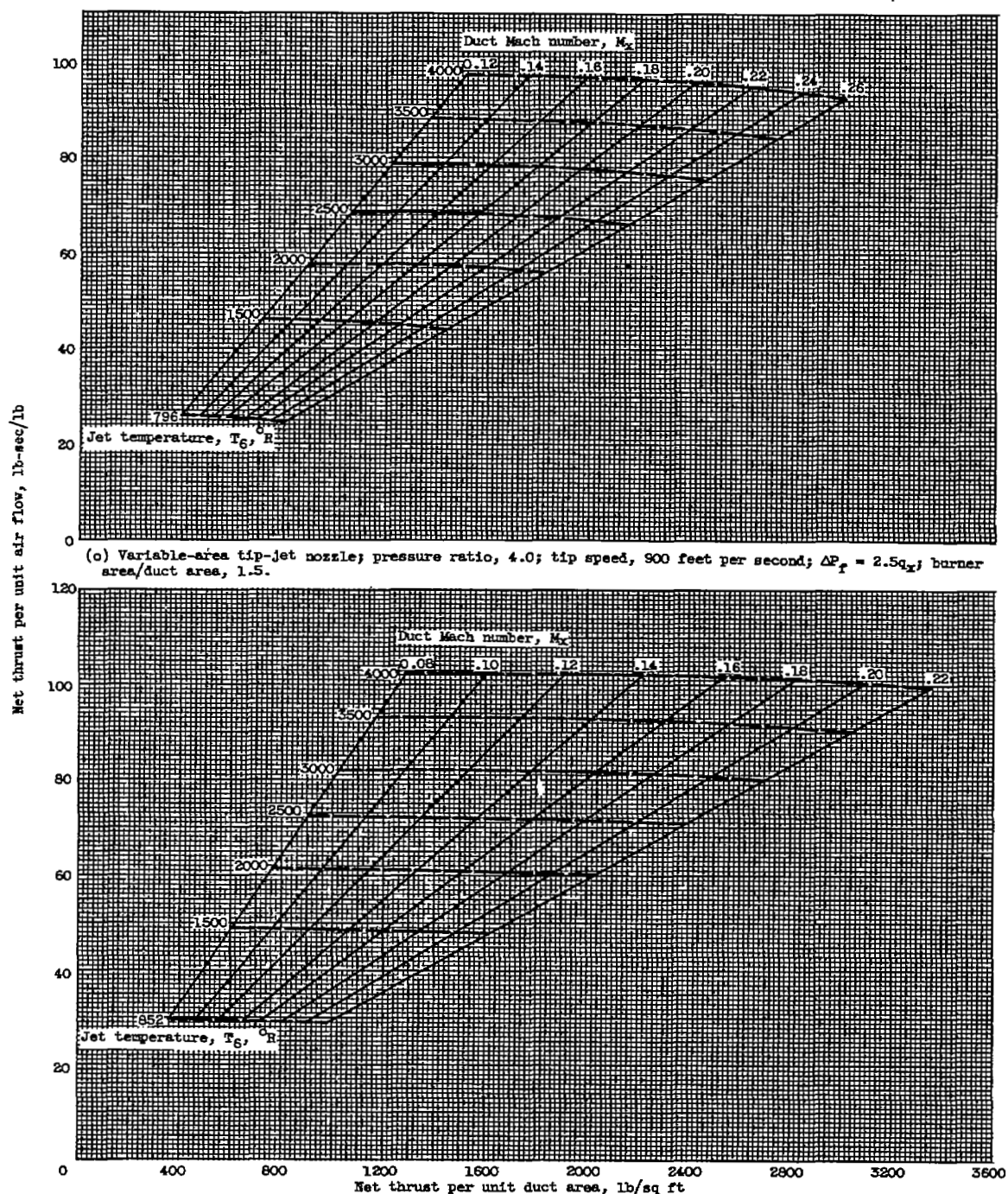
Figure 5. - Continued. Power-available chart.
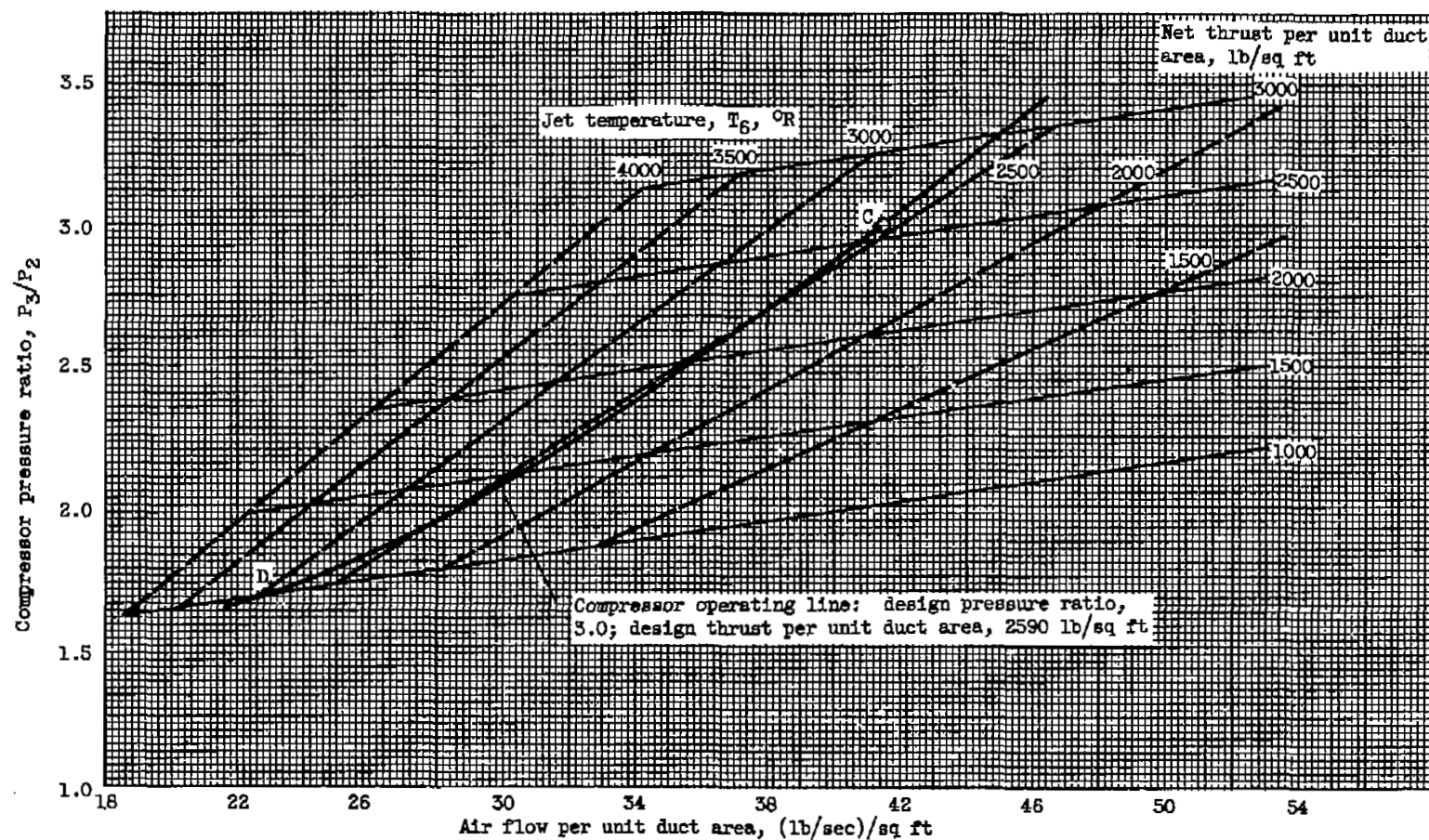
(q) Fixed-area tip-jet nozzle; tip speed, 700 feet per second; $\Delta P_f = 2.5q_x$; nozzle area/duct area, 0.6; burner area/duct area, 1.5.

Figure 5. - Concluded. Power-available chart.
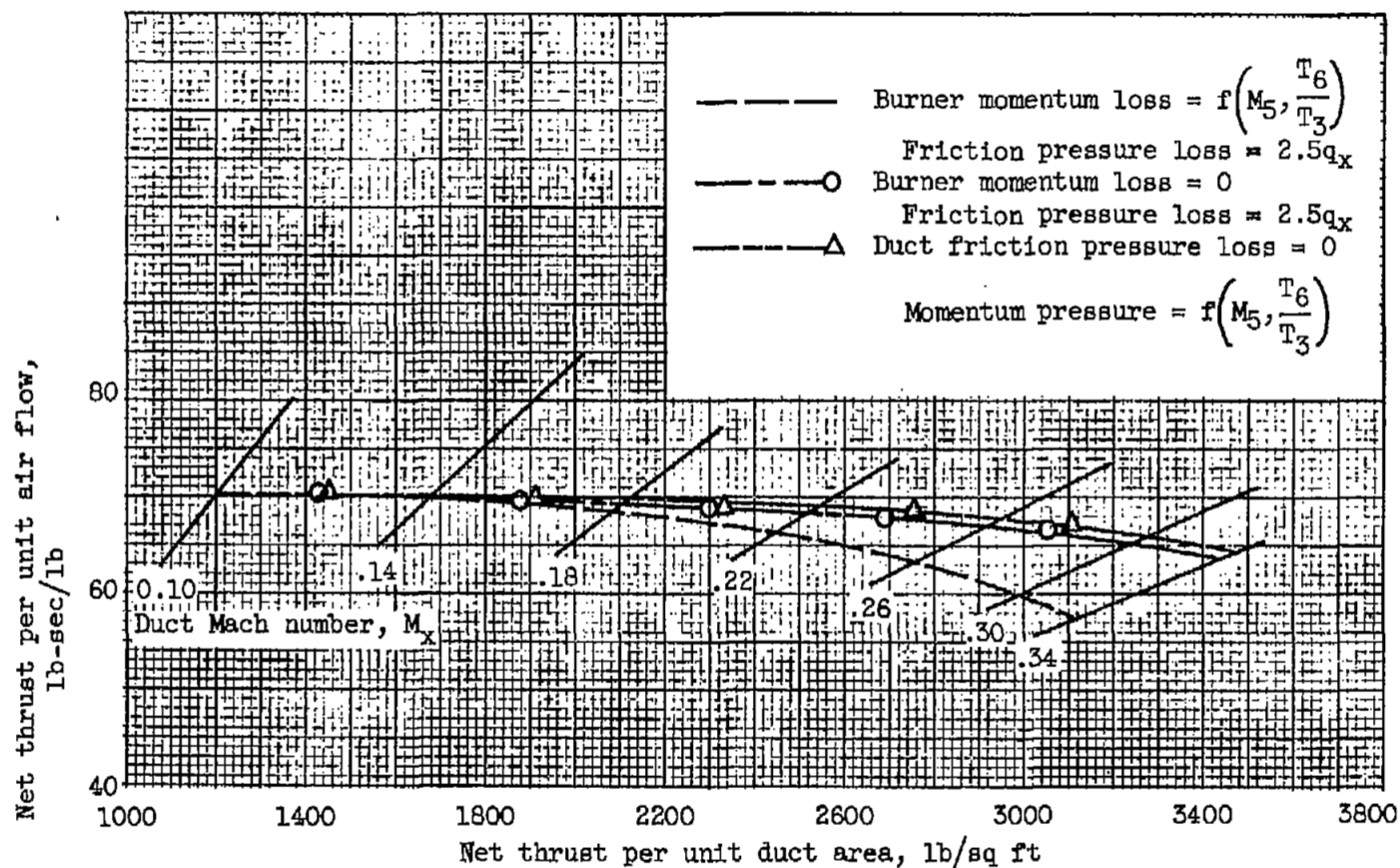
Figure 6. - Effect of duct friction pressure loss and burner momentum pressure loss on specific thrust. Pressure ratio, 2.5; tip speed, 700 feet per second; burner area/duct area, 1.5; jet temperature, 3000° R.
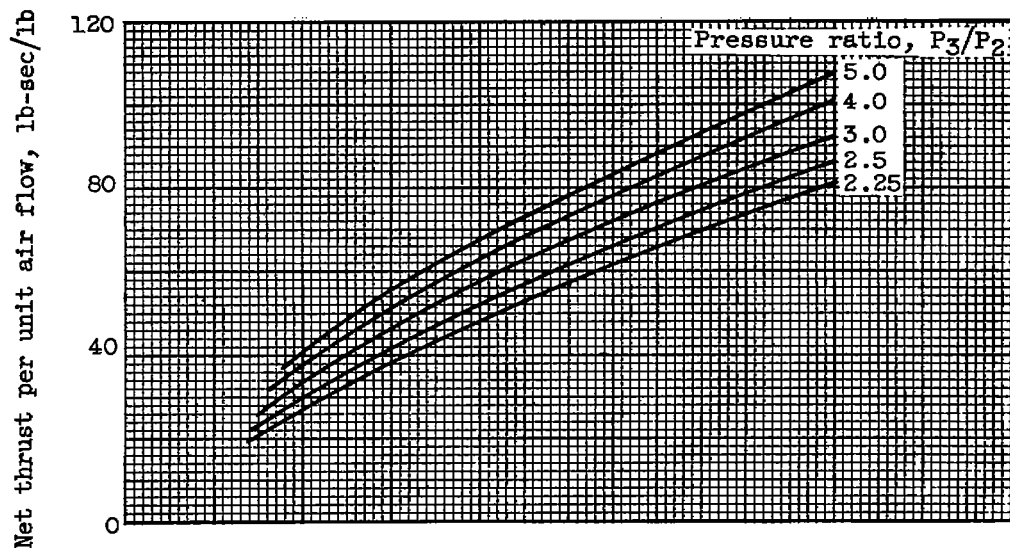
(a) Specific thrust.
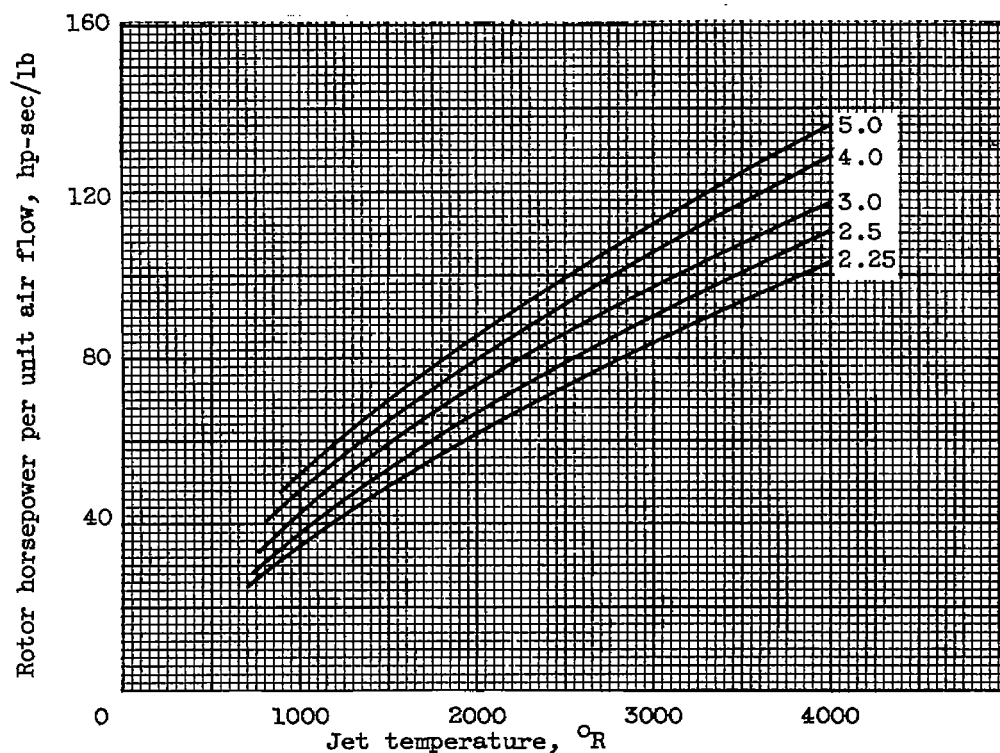
(b) Horsepower.

Figure 7. - Pressure-jet performance as function of
pressure ratio and jet temperature. Variable-
area tip-jet nozzle; tip speed, 700 feet per second;
burner area/duct area, 1.5; duct Mach number, 0.1.
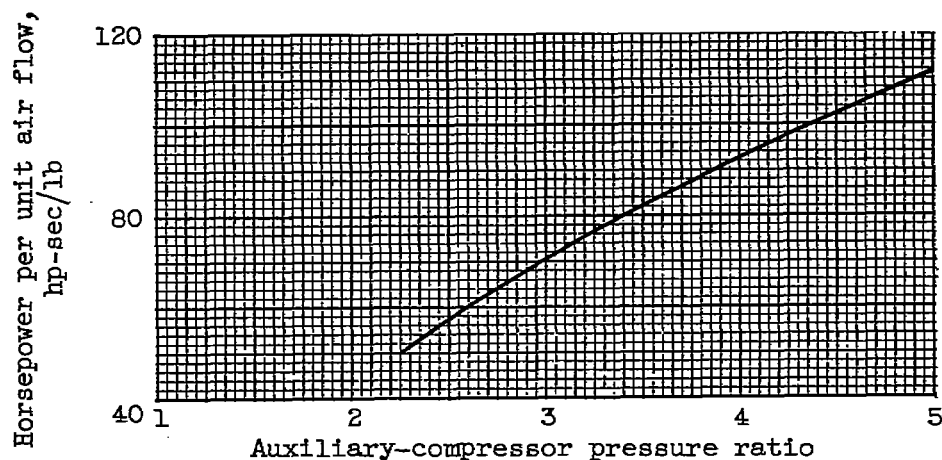
(a) Horsepower.
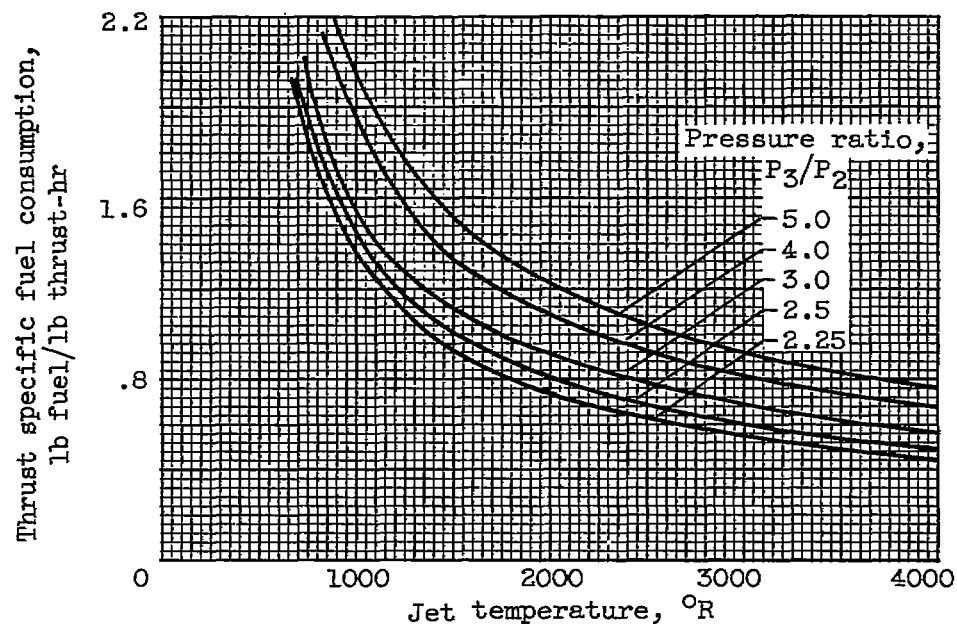
(b) Specific fuel consumption.

Figure 8. - Gas-turbine horsepower and thrust spe-
cific fuel consumption based on unit pressure-jet
air flow. Variable-area tip-jet nozzle; burner
area/duct area, 1.5; compressor efficiency, 0.87.
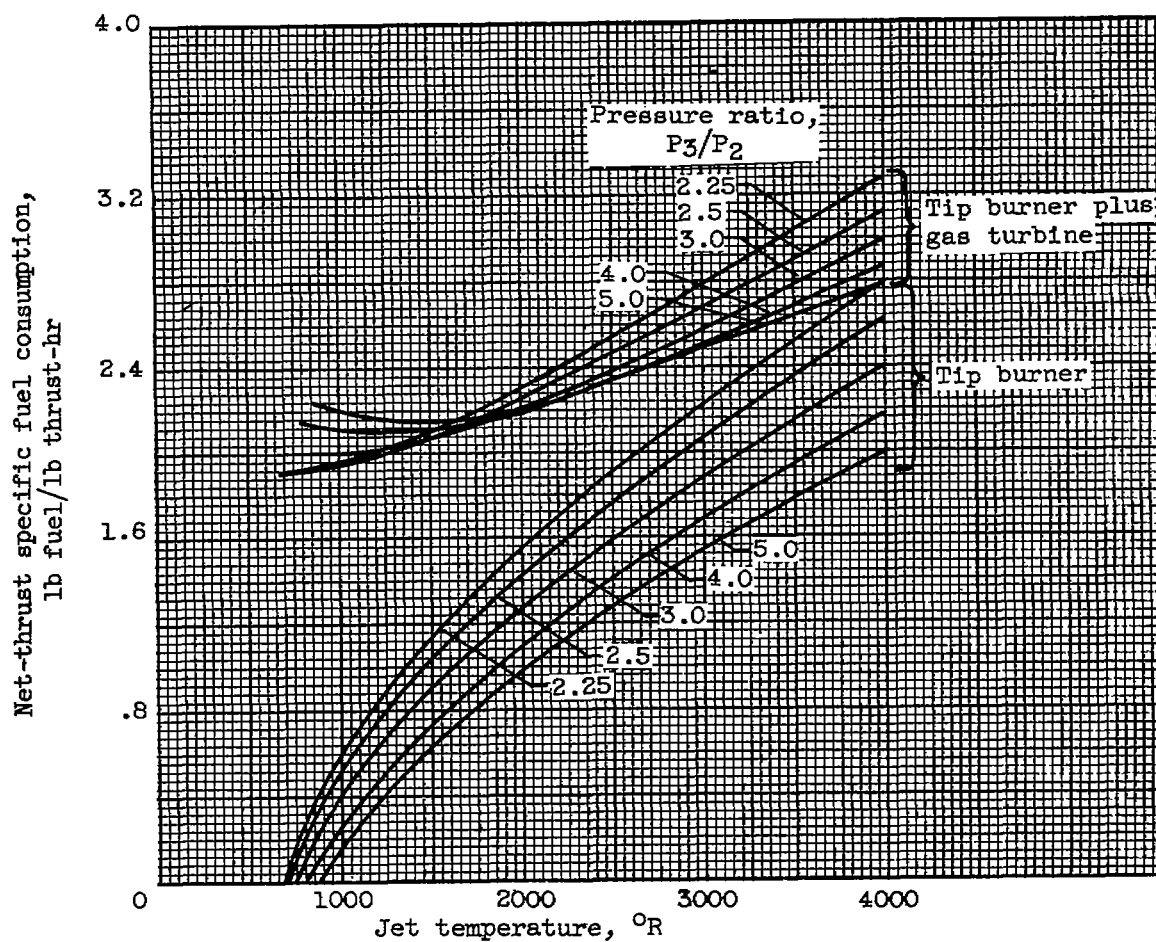
Figure 9. - Net-thrust specific fuel consumption of pressure jet. Variable-area jet nozzle; tip speed, 700 feet per second; burner area/duct area, 1.5; duct Mach number, 0.1.

3355

(a) Specific thrust.

(b) Horsepower.

Tip speed, ft/sec
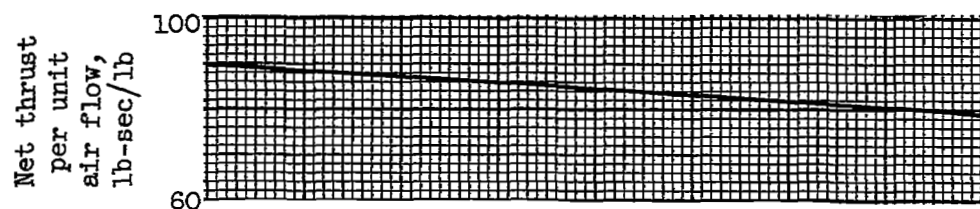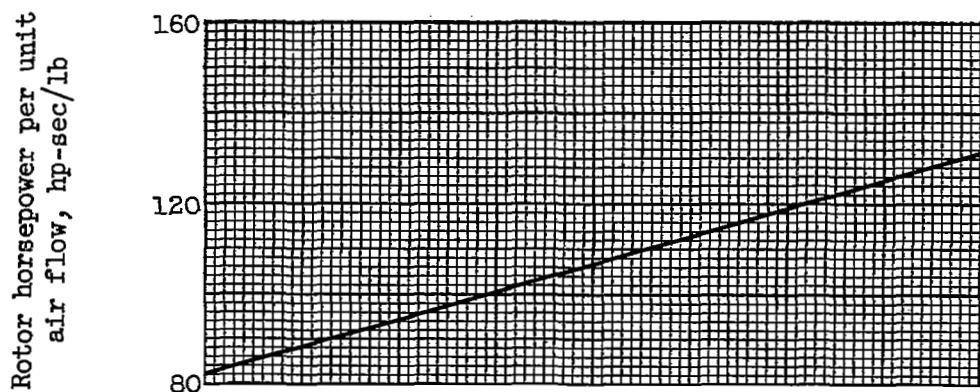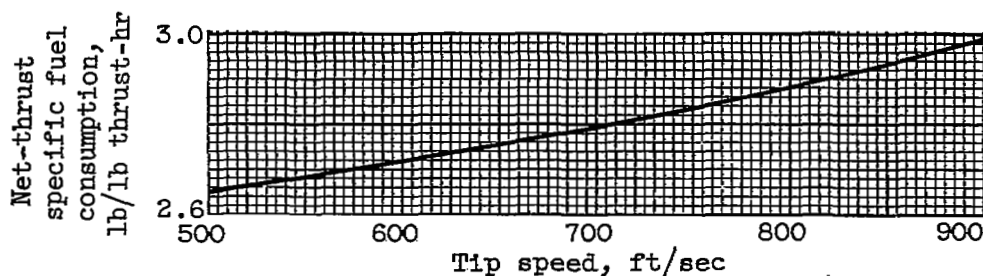
(c) Specific fuel consumption for gas turbine plus
    tip burner.

Figure 10. - Specific thrust, rotor horsepower, and
    thrust specific fuel consumption as functions of
    tip speed. Pressure ratio, 3.0; jet temperature,
    3500° R; burner area/duct area, 1.5; duct Mach
    number, 0.1.
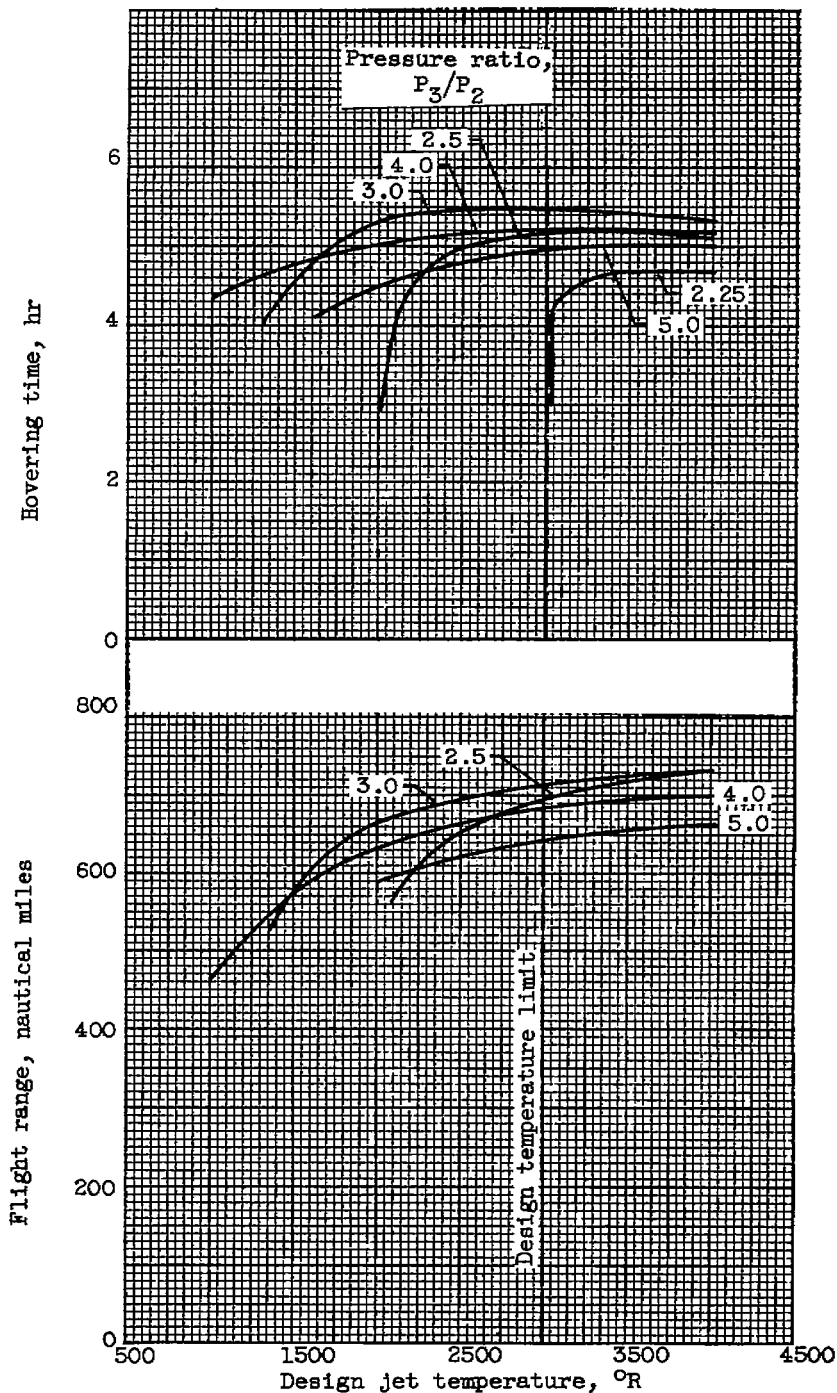
Figure 11. - Flight performance as function of design
jet temperature and pressure ratio. Tip speed, 700
feet per second; duct area, 0.3 × section area; burner
area, 0.45 × section area.
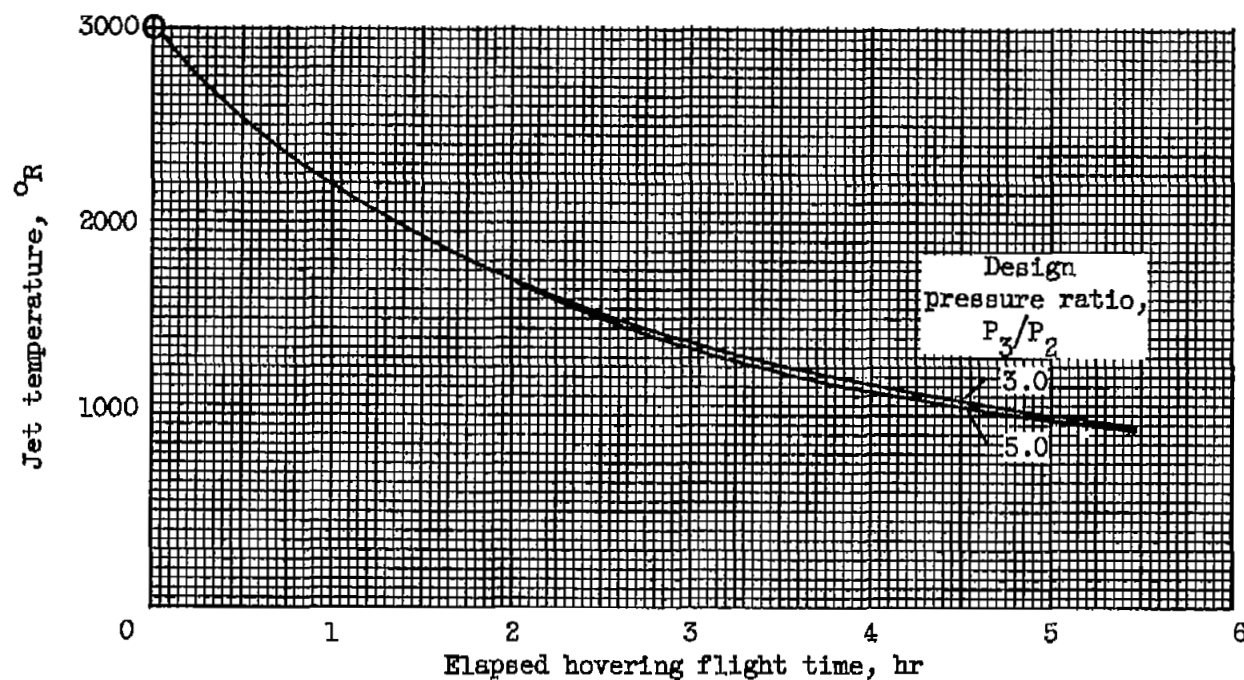
Figure 12. - Jet temperature as function of elapsed hovering time. Design jet temperature, 3000° R; tip speed, 700 feet per second; duct area/section area, 0.3; burner area/section area, 0.45.
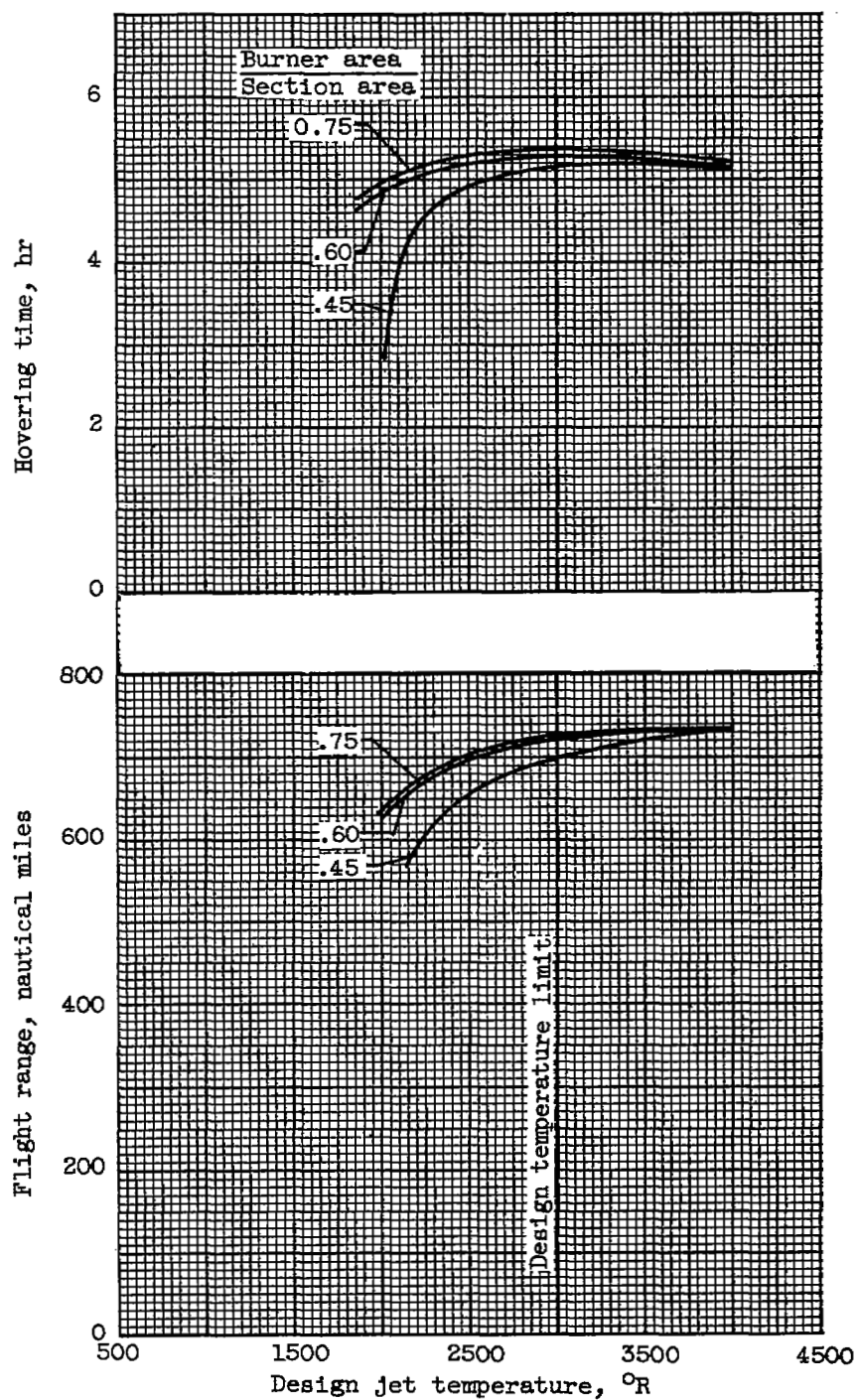
Figure 13. - Effect of burner area on flight performance.
Design pressure ratio, 2.5; tip speed, 700 feet per
second; duct area/section area, 0.3.

3355

.CQ-7 back
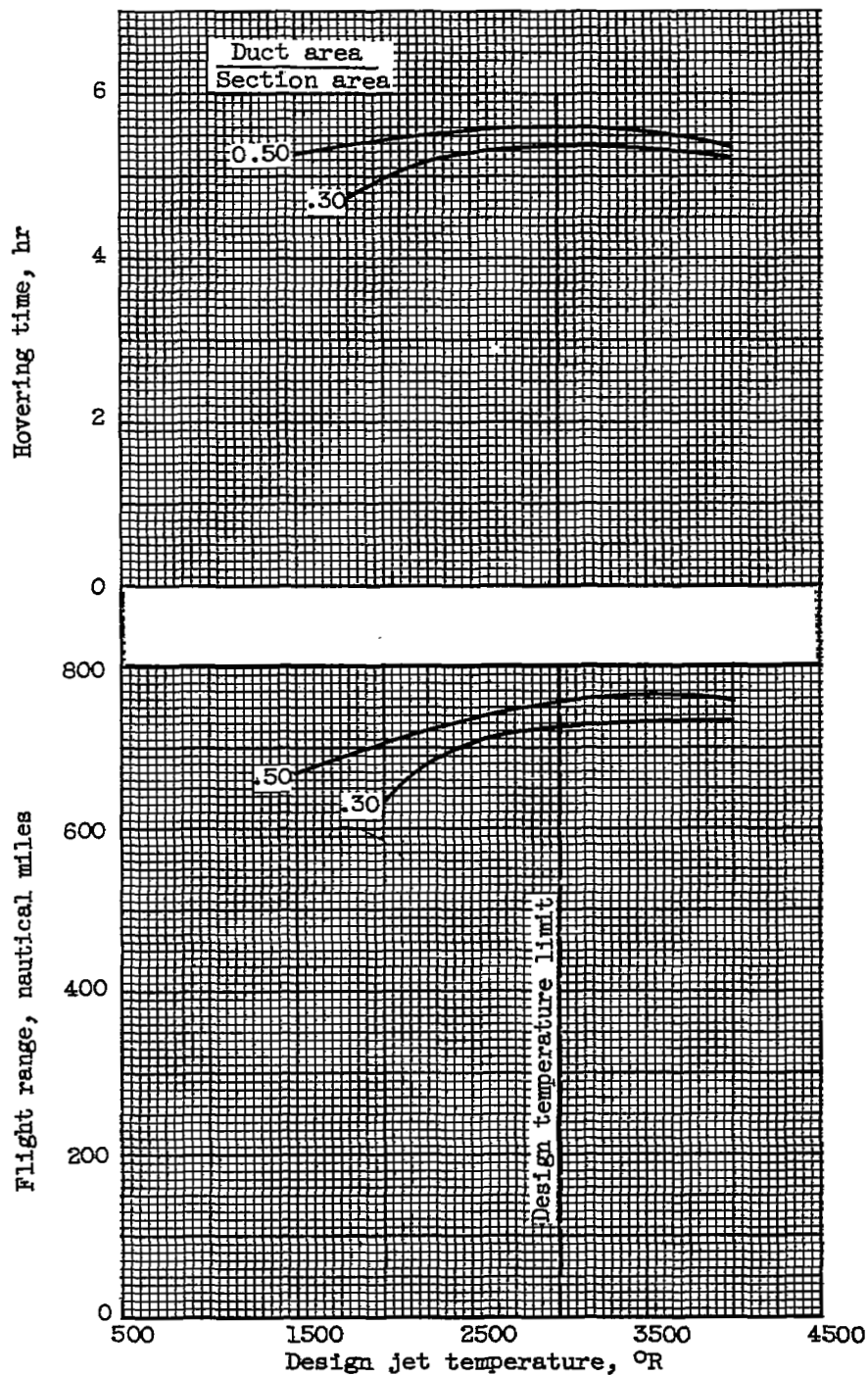
Figure 14. - Effect of duct area on flight performance.
Design pressure ratio, 2.5; tip speed, 700 feet per
second; burner area/section area, 0.75.
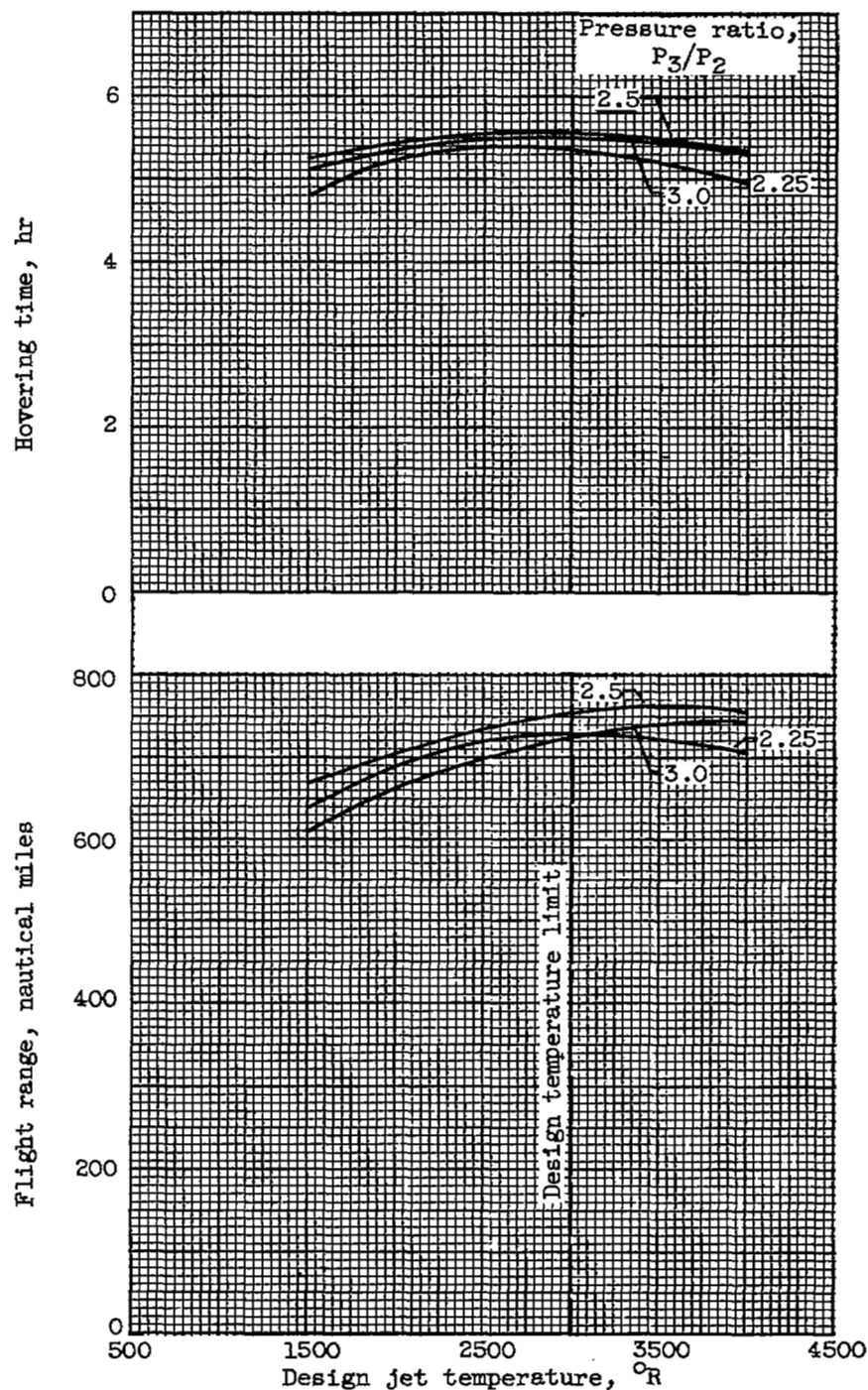
Figure 15. - Flight performance as function of design
jet temperature and pressure ratio. Tip speed, 700
feet per second; duct area/section area, 0.50; burner
area/section area, 0.75.
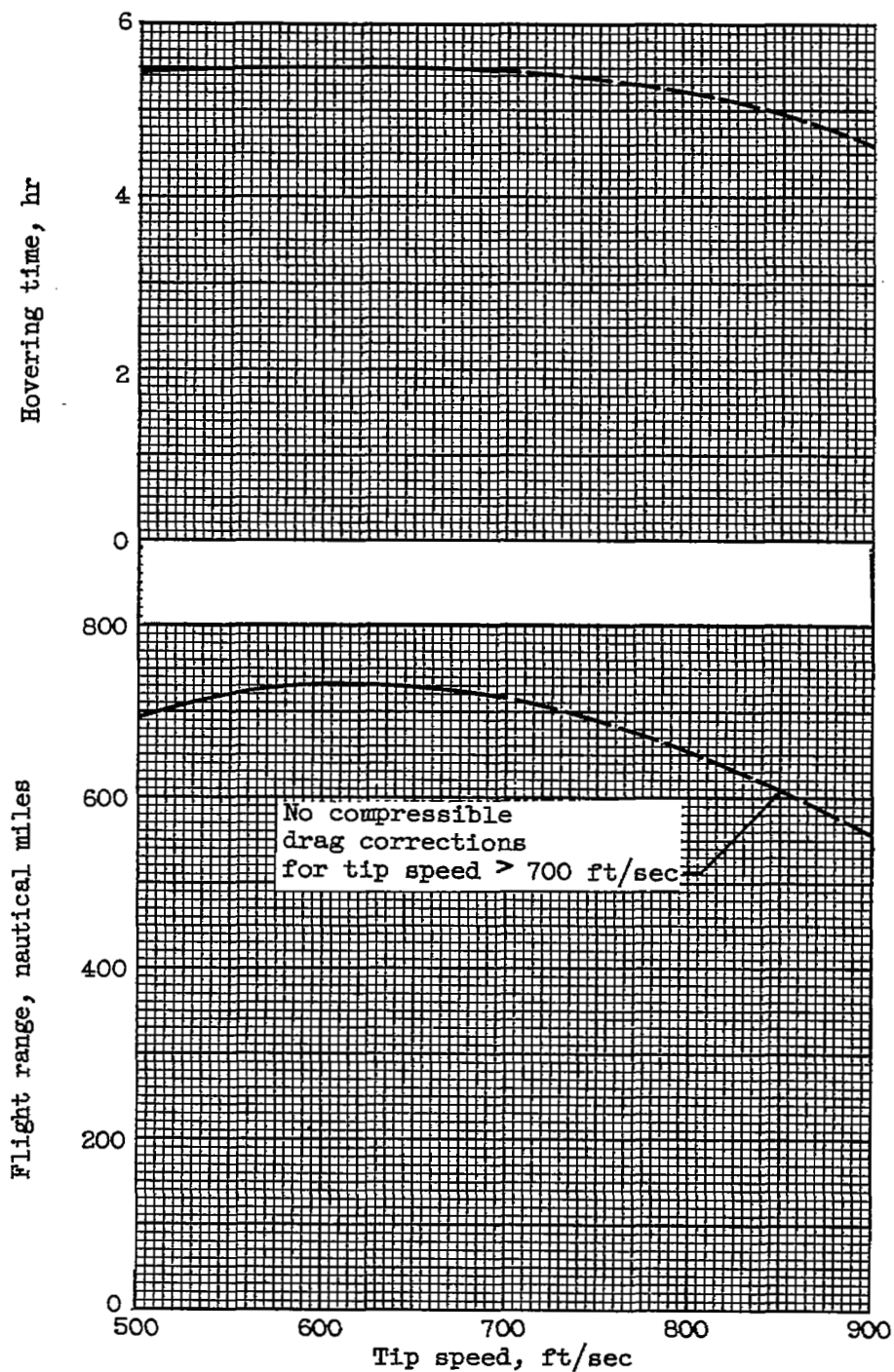
Figure 16. - Flight performance as function of rotor
tip speed. Variable-area tip-jet nozzle; duct
area/section area, 0.3; burner area/section area,
0.45.
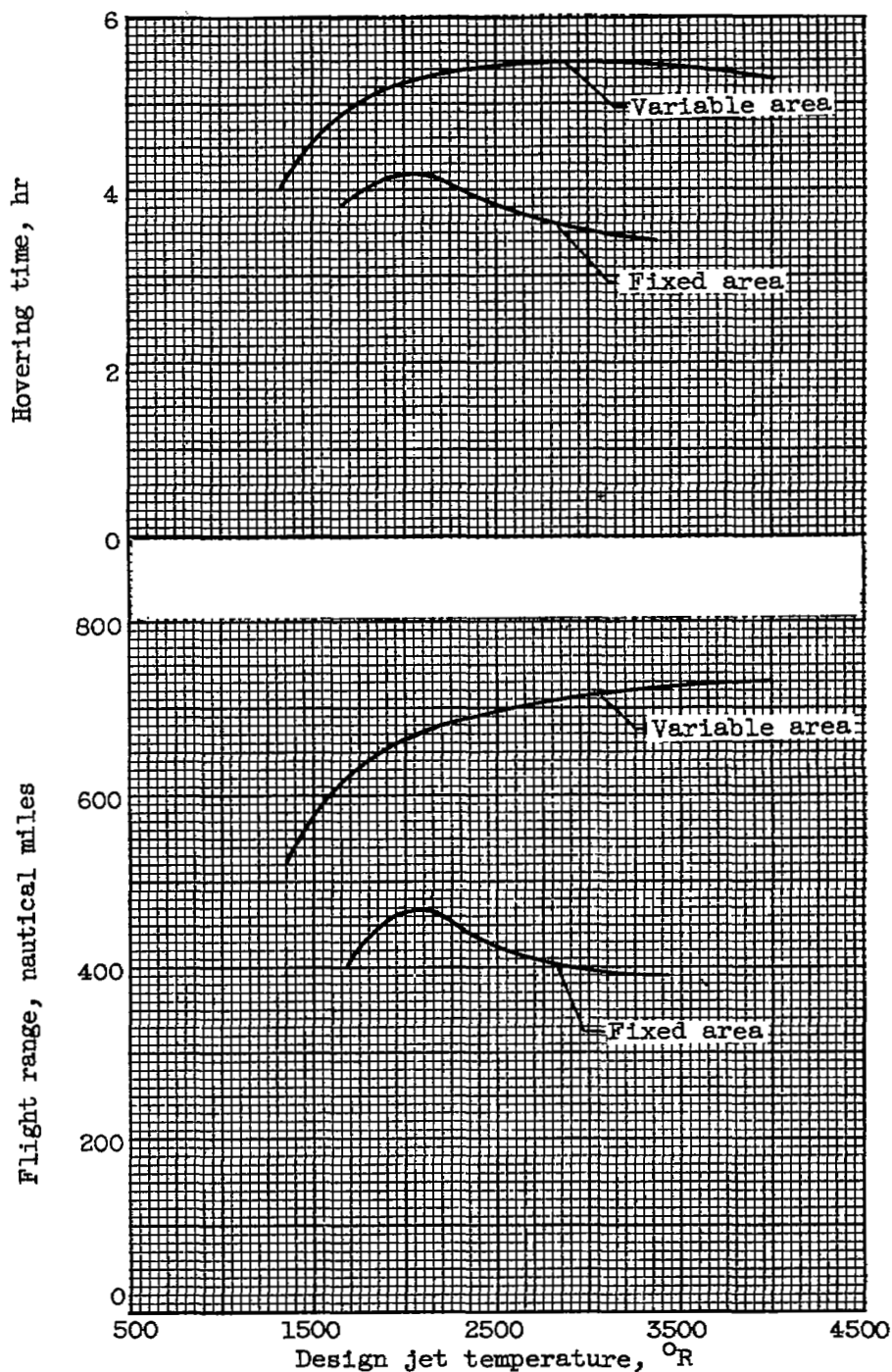
Figure 17. - Comparison of flight performance with variable- and fixed-area tip-jet nozzles. Design pressure ratio, 3.0; tip speed, 700 feet per second.
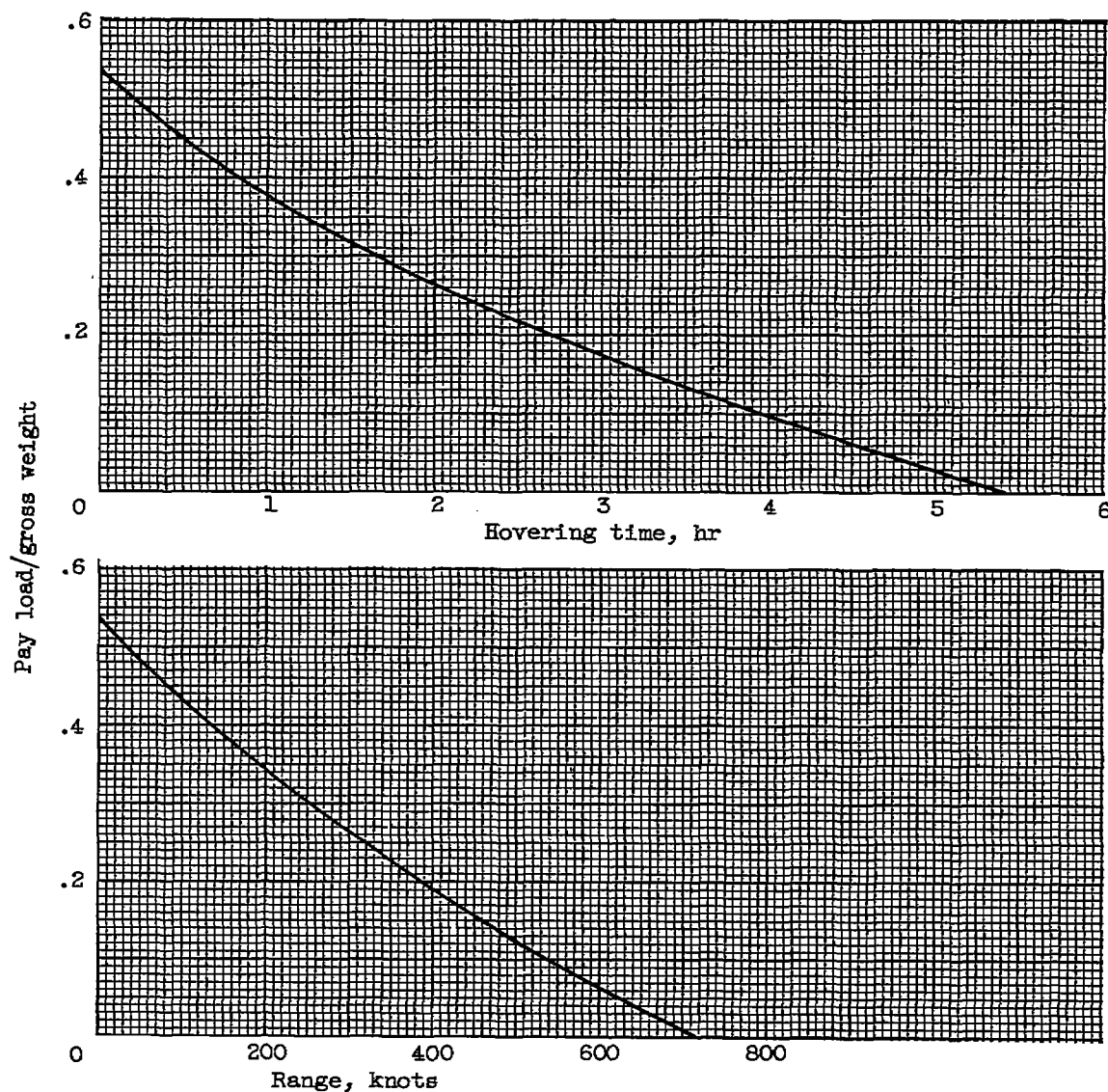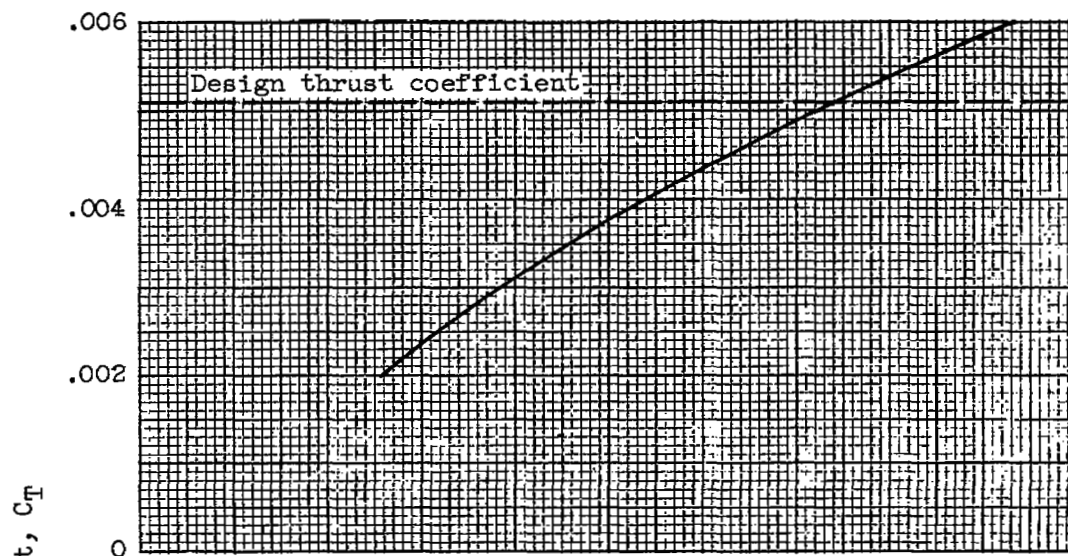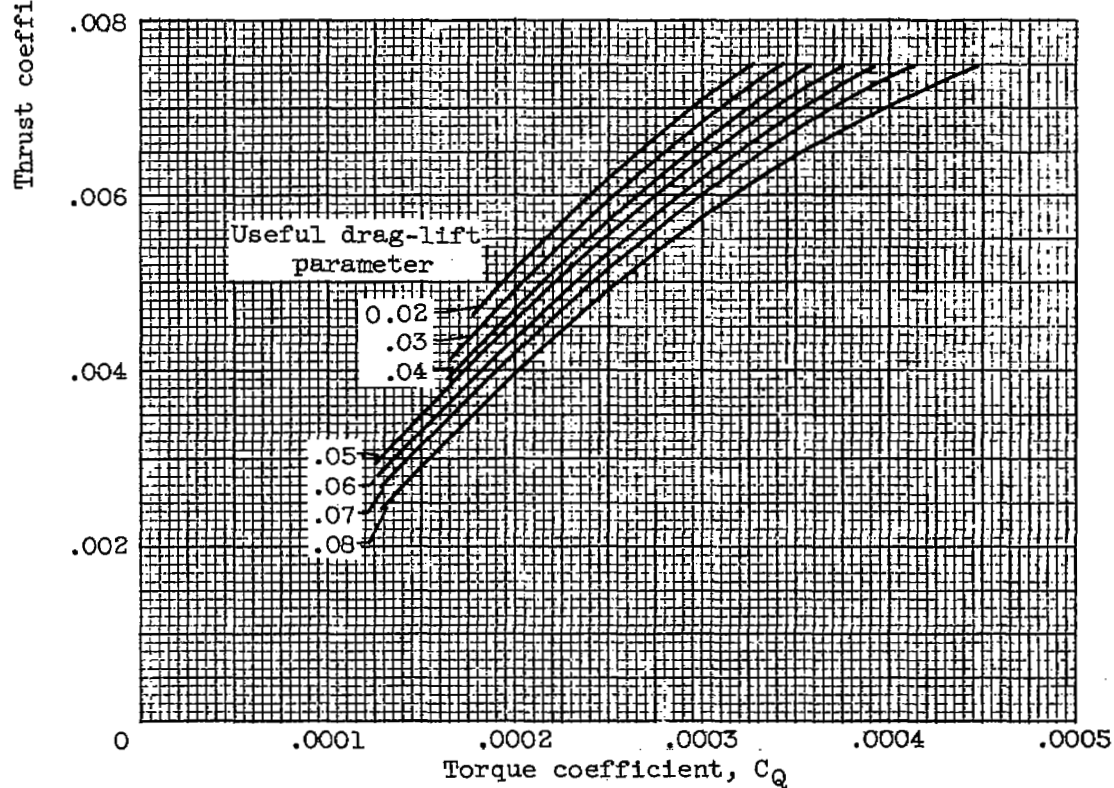
Figure 18. - Flight performance as function of pay load. Pressure ratio, 3.0; design jet temperature, 3000° R; tip speed, 700 feet per second; duct area/section area, 0.3; burner area/section area, 0.45.

(a) Hovering performance.

(b) Forward flight performance.

Figure 19. - Rotor performance in hovering and forward flight.
Airfoil, 64_1-012 (smooth); tip speed, 700 feet per second;
σ, 0.073.